Master's thesis

NTNU
Norwegian University of Science and Technology
Faculty of Natural Sciences
Department of Biology

Martine Drilsvik

The Function of Endomucin in Murine Hematopoietic Stem Cells

Master's thesis in Biotechnology
Supervisor: Kim Theilgaard-Mönch
Co-supervisor: Berit Johansen
June 2022

NTNU
Norwegian University of
Science and Technology

Martine Drilsvik

The Function of Endomucin in Murine Hematopoietic Stem Cells

Master's thesis in Biotechnology
Supervisor: Kim Theilgaard-Mönch
Co-supervisor: Berit Johansen
June 2022

Norwegian University of Science and Technology
Faculty of Natural Sciences
Department of Biology

NTNU
Norwegian University of
Science and Technology

Preface and Acknowledgements

The master's project was conducted in the Finsen Laboratory, Rigshospitalet and in the Biotechnology Research and Innovation Center, both Faculty of Health Sciences at the University of Copenhagen, Denmark. The project was part of a master´s program in Biotechnology devoted to molecular biology at the Norwegian University of Science and Technology (NTNU). The project started on September 1st, 2021, and lasted until the 10th of June 2022.

First and foremost, I would like to thank my supervisor at the Finsen Laboratory, Assoc. Prof. Kim Theilgaard-Mönch, for giving me the opportunity to contribute to an inspiring research group and carry out my master's project in the lab. I would also like to thank Prof. Berit Johansen who served as my supervisor at NTNU, for her guidance throughout this project. Furthermore, I wish to express my sincere gratitude to Assistant Prof. Kristian Reckzeh and PhD student Sophia Engelhard for their assistance throughout the project as well as their willingness to answer my countless questions. We carried out the project as a team, and without you it would not have been possible. I would like to thank all the members of the Theilgaard-Mönch group for making my days in the lab inspiring, it has been pleasure working with you. Finally, I wish to thank my friends, family, and partner for supporting me throughout the writing of this thesis.

Abstract

Hematopoietic stem cells (HSCs) are responsible for the lifelong production of all blood cells and are defined by their capacity to hierarchically reconstitute the entire blood system of a recipient following HSC transplantation. Due to this unique feature, HSC transplantation is used to treat various blood disorders, such as acute myeloid leukemia (AML). HSCs can be prospectively isolated based on their surface protein expression. However, to improve our understanding of HSC biology and to allow better assessment of HSC graft capacities, more sophisticated marker combinations are needed to further refine their immunophenotype. It has been reported that Endomucin (EMCN) is highly expressed on the surface of murine and human HSCs and that it enriches for immunophenotypic HSCs. Additionally, EMCN is not expressed by AML cancer cells, making the marker applicable for purifying tumor-free HSC grafts from AML patients for autologous transplantation. The latter statements make EMCN a promising new HSC marker. To investigate the function of EMCN in murine HSCs, a novel *Emcn* conditional knockout (KO) model was used to study the functional consequence of EMCN-loss on murine hematopoiesis. Following the induction of the KO, the frequency of peripheral blood (PB) cells, mature bone marrow (BM) cells, and HSCs was compared in the EMCN KO and the EMCN wild-type (WT) mice. HSC cell cycle analysis was also conducted before EMCN KO and EMCN WT HSCs were transplanted into lethally irradiated mice to study the effect of the KO on HSCs' repopulating capacity. Unfortunately, during experiments, it became evident that neither the EMCN KO mice nor the intended EMCN WT control mice expressed EMCN, and therefore, no differences could be expected between the two groups. However, the transplantation assays revealed that EMCN KO HSCs can regenerating the hematopoietic system of lethally irradiated recipients, indicating that EMCN is dispensable for the re-constitutional capacity of HSCs. However, to draw any conclusions regarding the function of EMCN in HSCs, the experiments need to be repeated with a proper EMCN WT control.

Sammendrag

Hematopoietiske stamceller (HSCs) er ansvarlig for den livslange produksjonen av alle blodceller og defineres av sin kapasitet til å rekonstruere hele blodsystemet til en mottaker etter HSC transplantasjon. På grunn av denne unike egenskapen brukes HSC transplantasjon som behandlingsform mot flere blodsykdommer, slik som akutt myelogen leukemi (AML). HSCs kan isoleres basert på deres overflateproteinuttrykk. Likevel, for å forbedre vår forståelse for HSC-biologi og for å tillate bedre vurdering av kapasiteten til HSC transplantat, trengs mer sofistikerte kombinasjoner av overflatemarkører slik at deres immunfenotype videre kan raffineres. Det har blitt vist at Endomucin (EMCN) er høyt uttrykt på overflaten til murine og humane HSCs og at HSCs er mer frekvent i cellepopulasjoner isolert basert på EMCN-uttrykk. I tillegg uttrykkes ikke EMCN på AML-kreft-celler som gjør at markøren kan brukes til å isolere AML-frie HSC-transplantat fra AML-pasienter for autolog transplantasjon. Dette gjør EMCN til en ny lovende HSC-markør. For å undersøke funksjonen til EMCN i murine HSCs, ble en ny betinget *Emcn* knock out (KO) modell brukt til å studere den funksjonelle konsekvensen av EMCN-tap i murin hematopoiese. Etterfulgt av induksjon av KO, ble frekvensen av perifere blod (PB) celler, modne beinmarg (BM) celler, og HSCs sammenliknet i EMCN KO mus og EMCN villtype (WT) mus. HCS cellesyklusanalyse ble også gjennomført, før EMCN KO og EMCN WT HSCs ble transplantert i dødelig bestrålte mus for å studere effekten av EMCN KO på HSCs sin rekonstruerende kapasitet. Dessverre ble det gjennom eksperimentene tydelig at hverken EMCN KO mus eller de tiltenkte EMCN WT musene uttrykte EMCN, og derfor kunne ingen forskjell mellom musene forventes. Likevel viste transplantasjonsforsøkene at EMCN KO HSCs kan regenerere the hematopoietiske systemet til dødelig bestrålte mus. Dette indikerer at EMCN ikke er essensiell for HSCs sin kapasitet til hematopoietisk rekonstruksjon. Til tross for dette må eksperimentene gjentas med en fungerende EMCN WT kontroll for at konklusjoner skal kunne trekkes angående funksjonen til EMCN i HSCs.

List of Abbreviations

AGM	Aorta-gonad-mesonephros
AML	Acute myeloid leukemia
ASCT	Autologous stem cell transplantation
BM	Bone marrow
bp	Base pair
CB	Cord blood
CDK	Cyclin-dependent kinase
CFSE	Carboxyfluorescein diacetate succinimidyl ester
CHIP	Clonal hematopoiesis of indeterminate potential
CIP/KIP	CDK2 interacting protein/kinase inhibiting protein
CKI	Cyclin-dependent kinase inhibitor
CLP	Common lymphoid progenitor
CMP	Common myeloid progenitor
CR	Complete remission
dNTP	Deoxynucleotide triphosphates
DNMT3A	DNA methyltransferase 3A
EC	Endothelial cell
EMCN	Endomucin
FACS	Fluorescence-activated cell sorting
FSC	Forward scatter
FMO	Fluorescence minus one
Gfi-1	Growth factor independent 1
G-CSF	Granulocyte-colony stimulating factor
GMP	Granulocyte-macrophage progenitor
gRNA	Guide RNA
GvHD	Graft-versus-host-disease
HGB	Hemoglobin
HLA	Human leukocyte antigen
HPC	Hematopoietic progenitor cells
HSC	Hematopoietic stem cell
HSPC	Hematopoietic stem and progenitor cell
IFN	Interferon

INK4	Inhibitor of CDK4
IDH	Isocitrate dehydrogenase
KO	Knock-out
LT-HSC	Long-term hematopoietic stem cell
mESCs	Mouse embryonic stem cells
MEP	Megakaryocyte/erythorid progenitor
MPP	Multipotent progenitor
NK	Natural killer
NPM1	Nucleophosmin 1
ns	Non significant
PB	Peripheral blood
PCR	Polymerase chain reaction
PolyI:C	Polyinosinic-polycytidylic acid
RBC	Red blood cell
RBE	Relative biological effect
RT	Room temperature
SSC	Side scatters
ST-HSC	Short-term hematopoietic stem cell
TF	Transcription factor
WBC	White blood cell
WBM	Whole bone marrow
WT	Wild type
YS	Yolk sac

Contents

1 Introduction

1.1 Hematopoietic stem cells and hematopoiesis

Hematopoietic stem cells (HSCs) are rare cells residing in the bone marrow (BM) of adult mammals and are responsible for producing and replenishing mature blood cells of all lineages [1]. This process is termed hematopoiesis, and the hematopoietic lineages include erythrocytes, platelets, granulocytes, macrophages, T cells, B cells, and natural killer cells (NK cells) [2]. Two defining properties of HSCs facilitate the life-long replenishment of the blood cells. These are their ability to self-renew and their potential to generate all lineages of blood, also referred to as multipotency. Self-renewal contributes to maintaining the hematopoietic stem cell pool in the BM, and their multipotency allows the HSCs to differentiate into a variety of hematopoietic progenitor cells (HPCs). Through specific and highly regulated pathways, the HPCs further develop into more lineage-restricted precursors. These precursor cells will gradually commit to mature blood cells [3].

1.1.1 Emergence of hematopoietic stem cells

For decades, researchers have been studying the hematopoietic system, and today, the hematopoietic system is one of the best characterized tissues in the body. [4]. Aiming to increase our understanding of HSCs and their role in human blood disorders and oncogenesis, extensive research has been conducted worldwide [5].

In vertebrates, hematopoiesis is initiated during embryonic development and continues throughout life. The HSCs are produced in the early embryo as distinct embryonic cells locate in specific hematopoietic sites during development. These sites represent different environments, termed niches, that facilitate HSC expansion and/or differentiation [1]. The first embryonic blood is produced during the first wave of hematopoiesis, termed the primitive wave. This takes place in the yolk sac (YS) blood islands, where the mesoderm gives rise to two types of hematopoietic progenitors termed the hemangioblasts and the hemogenic endothelium. In the YS blood islands, the hemangioblasts give rise to primitive HSC-like erythroid progenitors and angioblasts, which are the vascular progenitors of the endothelial cells [6]. The erythroid progenitors differentiate into red blood cells (RBC) and macrophages. The primary function of the first wave of hematopoiesis is

the generation of the red blood cells important for tissue oxygenation, which in turn are essential for rapid embryonic growth [1]. The primitive wave shows little HSC activity, and it is only transient. It is replaced by a second wave of hematopoiesis, the definitive wave which takes place in the embryo proper. During definitive hematopoiesis, HSCs, as well as blood cells representing all hematopoietic lineages, are produced. This process is commenced once the circulatory system is established, and through the vascular system, progenitor cells produced in the YS blood islands can migrate to other hematopoietic sites. In mammals, definitive hematopoiesis is initiated in the aorta-gonad-mesonephros (AGM) region of the embryo. Here, hemogenic endothelium gives rise to multipotent HSCs that, in turn, can differentiate into progenitor cells for all hematopoietic lineages. Together with progenitors produced in the YS blood islands, these cells colonize the fetal liver, where they expand and/or mature [6]. To expand the HSC pool, the HSCs undergo symmetrical division, where one HSC gives rise to two identical daughter cells possessing multipotency [7]. Ultimately, and prior to birth, they colonize the thymus, spleen, and bone marrow which provide distinct niches facilitating the expansion of HSC populations. In mammals, the BM serves as the primary hematopoietic niche throughout adulthood [1].

1.1.2 The hematopoietic system and its hierarchical order

During hematopoiesis, mature blood cells are produced to replenish all mature hematopoietic cell lineages. The different lineages have distinct functions in the body, making up a well-balanced and functional blood system [1]. The erythrocytes, or red blood cells, transport hemoglobin (HGB) carrying oxygen from the lungs to all tissues of the body before they return carbon dioxide to the lungs [8]. Blood platelets (PLT) are crucial for hemostasis as they prevent blood loss after injury by facilitating the formation of blood clots [9]. White blood cells (WBC), or leukocytes, are a heterogeneous population of immune cells protecting the body against pathogens, preventing infectious diseases. The WBCs comprise basophils, neutrophils, and eosinophils, which are all granulocytes, monocytes, and lymphocytes, including T cells, B cells, and NK cells [10]. Generally, mature blood cells are short-lived [1]. However, the lifespan of a blood cell varies among types of blood cells. For instance, in mice, the life span of erythrocytes is about 40

days [11], while murine neutrophils normally circulate in the blood for less than one day [12].

Due to the short lifespan of mature blood cells, the hematopoietic system needs to be highly dynamic in order to meet the constant requirement for new blood cells [13]. During steady-state hematopoiesis in mice, about 10^9 mature blood cells must be produced each second, and each cell type must be generated at different quantities [14]. To sustain such a dynamic process, HSCs are required throughout life.

Hematopoiesis can be depicted as a hierarchical system, with the HSCs at the apex of the hierarchy (Figure 1). Hematopoiesis is initiated by the activation of long-term HSCs (LT-HSCs), resulting in cell cycle entry. Upon entry, the LT-HSCs differentiate to produce short-term HSCs (ST-HSCs) [15], which further can differentiate into multipotent progenitors (MPPs). In contrast to LT-HSCs and ST-HSCs, the MPPs lack the potential to self-renew. Further, research indicates that as the MPPs differentiate they generate two lineage-committed progenitors including the common myeloid progenitor (CMP), and the common lymphoid progenitor (CLP) [16]. The CMP has the potential to differentiate into the myeloid blood cell lineages. This is initiated as CMP differentiation into the megakaryocyte/erythroid progenitor (MEP) and the granulocyte-macrophage progenitor (GMP), which further produce intermediate lineage-restricted progenitors. As these continue to differentiate, erythrocytes, platelets, granulocytes, and monocytes are produced [17]. The CLPs are the progenitors of the lymphoid lineages. They differentiate into the intermediate lineage-restricted progenitors Pro T, Pro B, and Pro NK, which ultimately gives rise to the lymphoid lineages producing mature T-cells, B-cells, and NK cells, respectively [18].

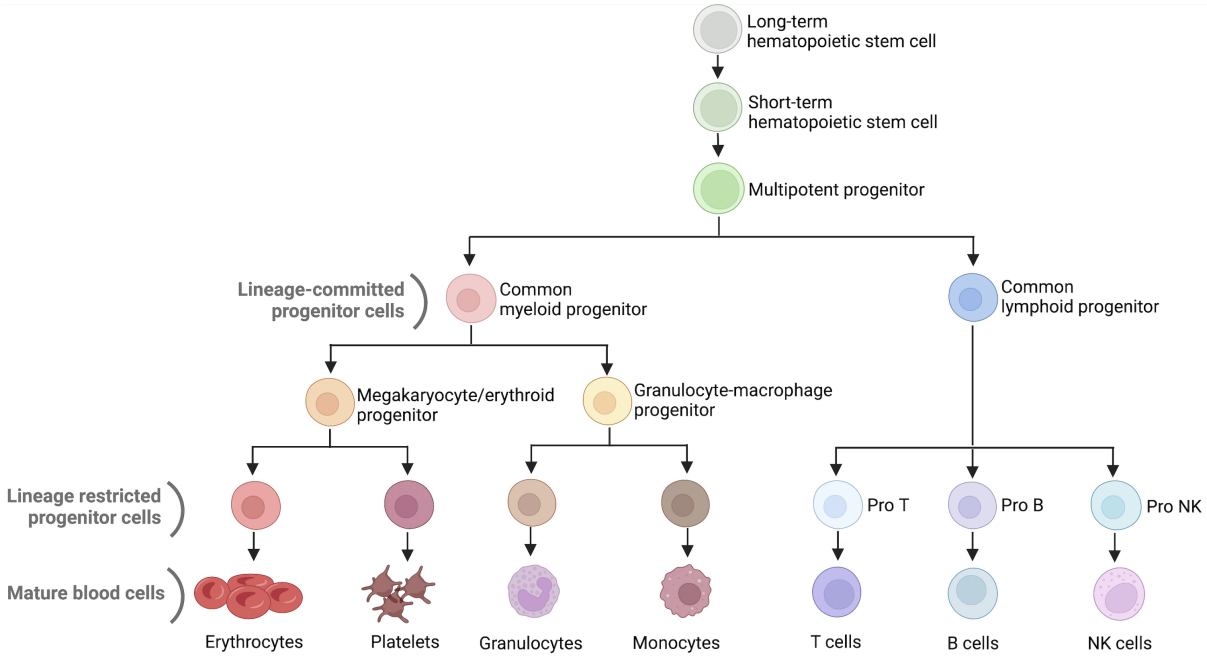

Figure 1: **The hierarchy of the hematopoietic system.** Upon cell cycle, LT-HSC produces ST-HSCs giving rise to MPPs. These further differentiate into lineage-committed CMP and CLP [16]. During a continuous process of differentiation, the CMP produces MEPs and GMPs, which through intermediate lineage-restricted progenitors produce erythrocytes, platelets, granulocytes, and monocytes [17]. CLP differentiate into the lineage-restricted proT, proB, and pro NK cells, giving rise to T cell, B cells, and NK cells, respectively [18]. Created with BioRender.com.

1.1.3 Hematopoietic cells are distinguished based on surface immunophenotype

Our current understanding of the relationship between HSCs, progenitor cells, and mature blood cells is based on the ability to prospectively isolate cell populations by fluorescence-activated cell sorting (FACS) and subsequently analyze these populations functionally through transplantation assays and cell cultures [19], [20]. Hematopoietic stem and progenitor cells (HSPCs), as well as mature blood cell lineages, express different sets of surface markers characteristic of the cell type, its level of self-renewal potential, differentiation, and lineage commitment [21]. Using monoclonal antibodiesa attached to fluorochromes to stain these markers, followed by FACS, unique cell surface protein expression patterns can be used to isolate cells from each developmental stage during hematopoiesis. [22].

The ability to characterize HSPCs and mature blood cells based on immunophenotypes does not only allow for in-depth studies of the hematopoietic system, but also for the enrichment of LT-HSCs, which allows for HSC-based regenerative therapies (discussed later) [23]. Populations of HSCs, as well as of lineage-committed progenitor cells, such as MEPs and GMPs, have been defined on the basis of surface markers allowing for their isolation. However, these populations are not pure. Especially MPPs and HSCs are challenging to purify because they express surface markers that are characteristic for distinct lineages. This phenomenon is termed lineage-priming and proposes that lineage specification is a process where lineage fates are gradually excluded as the cell progress towards one specific lineage [1].

At present, no HSC surface marker has been identified that may be used alone for LT-HSC purification. In order to enrich for LT-HSC, several markers have been combined, and today a variety of antibody staining panels are used [21]. Most of the staining panels used for murine LT-HSC purification rely on HSCs' surface expression of c-Kit and Sca-1, and the absence of markers expressed on mature blood cells (i.e., CD11b, Gr-1, CD3e, Ter-119, and B220) [24]. In adult mice, this cell population, generally referred to as LSK (**L**ineage$^-$ **S**ca-1$^+$ c-**K**it$^+$), contain all the multipotent cells. However, the majority of LSKs represent progenitor cells, and only about 10% of the LSKs are LT-HSCs [21]. To further enrich for the murine LT-HSCs, cells negative for CD34 can be selected [25]. Another approach is to select cells that express CD150 while being CD48 negative [26]. CD150 expression correlates with the LT-HSCs' capacity to self-renew and reconstitute hematopoiesis after transplantation, which declines as CD150 expression levels decrease. The MPPs can be isolated from the LSKs based on their absence of surface CD150 and the presence of CD48. However, despite surface markers and advanced staining and sorting strategies aiming for optimal purification, HSC and MPP populations still show great heterogeneity [27].

Distinct surface expression patterns also allow for the isolating of mature blood cell populations. It is known that mature blood cells express markers that are critical to their immune reactions, and these markers can be used to isolate mature blood cells efficiently. Evidence show that mature B cells, myeloid cells, and T cells express B220,

Gr-1/CD11b [21], and CD3e [24], respectively. Upon antibody staining followed by FACS, these markers are used to isolate B cells, myeloid cells, and T cells in peripheral blood (PB) and BM [21].

1.1.4 Flow cytometry

Flow cytometry instruments have been under development since the 1960s when they first evolved, and during the past decades, their use in clinical laboratories has grown considerably [28], [29]. Since then, the flow cytometers have developed from only being able to measure cell size to the current instruments, which enable the counting and sorting of cells based on 14 distinct parameters. Inside the flow cytometry instrument, cells (or other particles) are separated in a fluid stream enabling single cells to pass through a light source (usually a laser). Parameters like cell size, granularity, and fluorescence of bound fluorochrome-conjugated antibodies can be measured as light scatter and fluorescence emission, which allows the distinction of cell populations [28].

Light scatter, referring to the light deflected around the cell as the laser light strikes it, can be divided into two types: side scatters (SSC) and forward scatter (FSC). Refracted and reflected light measured 90 degrees to the laser beam is termed SSC, which is used to determine the internal complexity of the cell, e.g., granularity. FCS, however, is diffraction measured along the laser beam axis and can be used to determine cell size [30].

By using flow cytometry, a variety of cell surface and intracellular antigens can be identified. Intracellular components (e.g., DNA) can be stained with fluorescent dyes, and surface or cytoplasmic proteins can be stained using fluorochrome- conjugated antibodies. As a laser beam strikes cells stained with fluorochromes, the fluorochromes are excited, which eventually results in the emission of light that can be detected [29]. Because current flow cytometers generally have several lasers, and because a variety of fluorochromes emit light at different wavelengths (even when excited with the same laser), multicolor staining panels can be used to identify patterns of surface or intracellular proteins in an experiment [31]. FACS are flow cytometers possessing the capacity to sort distinct cells of a mixed cell population stained with fluorochromes [28].

Inside a flow cytometer, optics collect emitted light and direct it to optical filters and dichroic mirrors. These allow the isolation of specific wavelength bands, which further are detected by photomultiplier tubes and digitized for computer analyses [28].

1.2 Regulation of hematopoietic stem cells

1.2.1 HSC self-renewal and differentiation is balanced in hematopoiesis

The number of HSCs that can be isolated from the bone marrow of an individual mouse depends on sex, age, strain, and the purification strategy. However, Kiel et.al., has demonstrate that only about 0.005% of whole bone marrow cells are immunophenotypic HSCs (LSK $CD150^{+}CD48^{-}$) [32]. To preserve homeostasis while these rare cells replenish blood cells as they are turned over or lost, the HSC population size must remain steady [33]. During steady-state hematopoiesis, this is accomplished by a delicate balance between HSC self-renewal and HSC differentiation upon mitosis, facilitated by a process known as asymmetrical cell division. Asymmetrical cell division is carried out either by asymmetrical self-renewal (divisional asymmetry) or by environmental asymmetry. During asymmetrical cell division, cell-fate determinants are unevenly distributed upon mitosis, whereas in environmental asymmetry, one of two identical HSC daughter cells migrates from the HSC niche to an environment that facilitates differentiation. Both processes result in one daughter cell that retains the HSC fate, whereas the other daughter cell undergoes differentiation [34]. During hematopoietic stress, for example, caused by infection, symmetrical HSC division might be necessary in response to extensive demands for new blood cells [35]. Symmetrical division either results in two new HSCs or two differentiating daughter cells [36].

During steady-state hematopoiesis, 90-95% of the HSCs are quiescent, referring to a state where the cells do not divide. This facilitating the life-long maintenance of the HSC population size, as well as steady myeloid and lymphoid output (Figure 2). However, research has shown heterogeneity in the quiescent HSC population allowing the distinction between a dormant and an active sub-population. Although the mechanisms regulating the quiescent state of the HSCs are not fully known, research has revealed that

the dormant HSCs have long-term re-constitutional potential. The dormant HSCs serve only as a reserve pool for maintaining homeostasis in response to hematopoietic stress. In response to hematopoietic stress, these cells will exit the quiescent state, proliferate, and differentiate to meet the increased demands for mature blood cells. In contrast, the active sub-population sustains the HSC population during homeostasis and ensures production of an adequate number of differentiated blood cells [37]. Quiescent cells are in the G_0 phase of the cell cycle, where the cells do not divide. However, this state is reversible upon stimulation, as the HSCs possess the ability to enter G_1 phase (interphase). The cells can further progress through G_1, S phase (DNA synthesis phase), G_2 (interphase), and M phase (mitosis phase) of the cell cycle, and thus proliferate [38]. During homeostasis, about 5 percent of the HSCs are actively in the cell cycle [37].

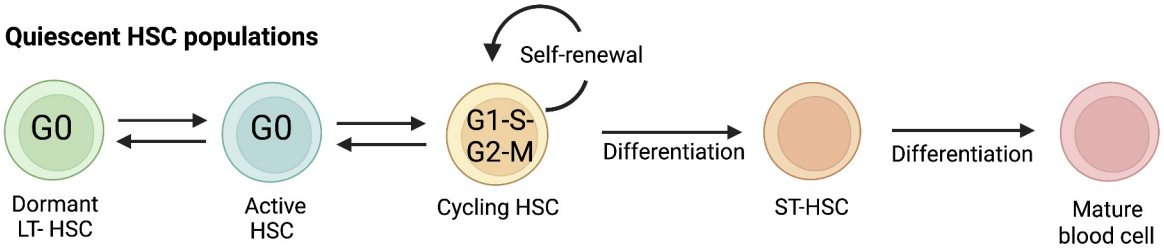

Figure 2: **Quiescent HSCs can enter cell cycle and differentiate upon activation.** Activated HSCs can enter and proceed through cell cycle (G_1 phase, S phase, G_2 phase, and M phase) to differentiate, or to self-renew [38]. Differentiating HSCs gradually lose their life-long self-renewal potential resulting in short-term HSCs (ST-HSCs) that can further differentiate to produce lineage-specific blood cells. Upon cell cycle entry, HSCs also have the potential to exit the cell cycle and enter to a dormant state [39]. Modified from [39], created with BioRender.com.

1.2.2 HSC fate is controlled by HSC extrinsic and intrinsic factors

Generally, HSCs have several developmental options; they can remain quiescent, self-renew (symmetrically or through asymmetrical cell division), differentiate, migrate, or undergo programmed cell death (apoptosis) [40]. In order for the hematopoietic system to maintain a balance between self-renewal and differentiation during steady-state hematopoiesis and in response to hematopoietic stress, cell fate decisions must be care-

fully controlled. Cell fate is determined by gene expression patterns and cell cycle status, which is regulated by a complex network of mechanisms. These include a complex interplay between extrinsic regulatory mechanisms of the BM microenvironment and niche, and the intrinsic regulatory mechanisms of HSCs [37].

The hematopoietic stem cell niche and extrinsic mechanisms

In the BM, HSCs are localized in specialized compartments called stem cell niches. In the niche microenvironment, HCSs are maintained and regulated through their interaction with other BM cells (e.g., endothelial cells, osteoblasts, and stromal fibroblasts), the extracellular matrix (ECM), and through receptor ligands [41]. The HSC niche consists of the endosteal surface, called the osteoblast niche, and the sinusoidal endothelium, which makes up the vascular niche (Figure 3) [42]. It is believed that the osteoblast niche facilitates HSC quiescence, which is important for maintaining the HSC pool, while the vascular niche offers a suitable environment for cycling HSPCs. Whether these two environments represent two distinct niches or if they are sub-compartments of a single niche is still debated [43]. Furthermore, quiescent LT-HSCs are frequently situated in less oxygenated, or hypoxic, niches which protects them from damage caused by reactive oxygen species [44]. The HSCs are anchored to the niche cells through adhesion molecules such as integrins and cadherins. The LT-HSCs also express calcium-sensing receptors, which in addition to the adhesion molecules, enable them to position in the osteoblast niche where the calcium concentration is higher compared to in the vascular niche. [45]. Close physical proximity to the niche facilitates paracrine signaling between the microenvironment and the HSCs. Such signaling involves cytokines and growth factors expressed on the surface or secreted by niche cells [46].

According to research, the osteoblastic niche's ability to maintain the HSC pool by facilitating quiescence is dependent on osteoblastic cells (OBs) on the endosteal surface [47]. Interaction with OBs maintains the HSCs localization in the osteoblastic niche, and the OBs express several activating regulators of LT-HSCs. Among these are the stem cell factor (SCF), angiopoietin 1 (Ang-1), and thrombopoietin (TPO), which bind to the HSC surface receptors c-kit, Tie2, and MPL, respectively [45]. There are also a variety of factors known to inhibit HSCs. Among these are the Transforming growth factor-β

(TGF-β), which can be found in a secreted form in the BM. TGF-β suppresses HSC activity via SMAD signaling downstream of TGF-β [48].

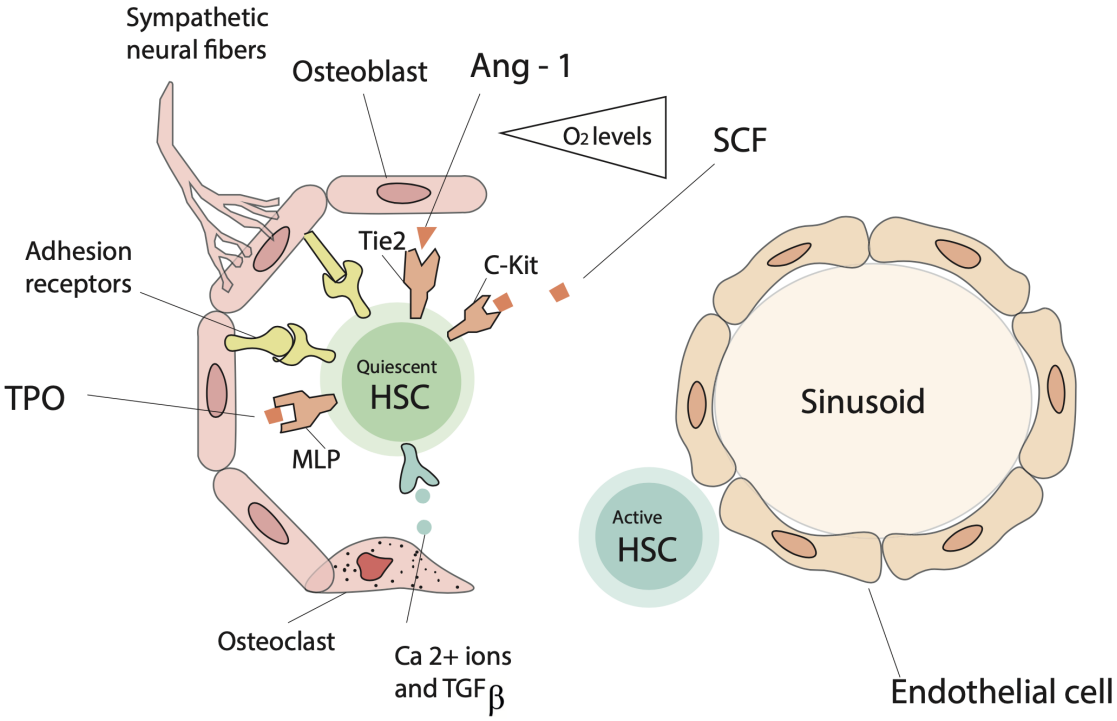

Figure 3: **The HSC niche simplified.** The HSCs are localized in BM niches, where they receive signals from niche cells (endothelial cells, osteoblasts, and stromal fibroblasts), ECM, and receptor ligands regulating quiescence and differentiation [41]. The osteoblast niche is thought to facilitate HSC quiescence through positive regulators such as SCF, Ang-1, and TPO, which signals through the receptors c-kit, Tie2, and MPL, respectively [45]. However, TGF-β suppresses HSC activity [48]. The osteoblast niche provides a hypoxic environment facilitating HSC quiescence [44]. Calcium receptors on the HSCs enable them to position in the osteoblastic niche where the calcium level is high compared to the surroundings [45]. Adhesion molecules presented on the niche cells also facilitate HSC positioning in the niche. The sinusoidal endothelium makes up the vascular niche which is thought to provide suitable conditions for cycling or active, HSCs [43]. Modified from [43], created with Adobe Illustrator.

Extrinsic mechanisms permit communication between the microenvironment and the HSCs' intrinsic factors. This allows HSCs to respond to increased demands for more mature blood cells, for example following bleeding, infection, or activation of an inflam-

matory response. Depending on the hematopoietic demand signaled from the niche, HSCs can adjust to ensure the best possible response [37]. A signaling pathway set in motion by extrinsic cues can, for example lead to changed gene expression, resulting in down-regulation of regulators involved in maintaining HSC quiescence [38].

HSC intrinsic mechanisms

Through extensive studies, a variety of different intrinsic factors regulating HSC fate have been discovered [37]. The core apparatus that regulates cell cycle during hematopoiesis includes the cyclin-dependent kinases (CDKs), which contribute to cell cycle progression [38]. The CDKs belong to a family of serine/threonine protein kinases, and upon activation, they bind cyclin regulatory subunits [49]. Through competing actions, the CDK/cyclin complexes are regulated by CDK inhibitors (CKIs), which facilitate hematopoietic "stemness" by preventing cell cycle progression [50].

A variety of CDKs are known to drive HSCs through cell cycle, and as different cyclins are expressed at different cell cycle stages, specific CDK/cyclin complexes are made as the cell proceeds through each of the cell cycle phases [37]. CDK4 and CDK6 bind cyclin D and control early to middle progression through G_1 phase. To further proceed, the cell express cyclin E in late G1 phase, which binds to CDK2, facilitating the transition from G1 to S phase. Further, and dependent on the cyclin expression in each phase, CDK2 and CDK1 drive HSCs through S, G_2, and M phase of the cell cycle, respectively [38].

The activity of the CDK/cyclin complexes can be blocked by CKIs. CKIs therefore plays a critical role in balancing the HSC pool and the hematopoietic demand during homeostasis and hematopoietic stress [51]. Generally, there are two main families of CKIs, namely the INK4 (Inhibitor of CDK4), and the CIP/KIP (CDK2 interacting protein/kinase inhibiting protein) family. The INK4 family includes $p15^{INK4b}$, $p16^{INK4a}$, $p18^{INK4c}$, and $p19^{INK4d}$, whereas the CIP/KIP holds the $p21^{CIP}$, $p27^{KIPI}$, and the $p57^{KIP2}$ of CKIs. Upon diverse signals, CKIs block the actions of the CDK/cyclin complexes at different stages of the cell cycle [37]. Furthermore, research has revealed several transcription factors (TF) that regulate HSC quiescence. It has been shown that a variety of TFs, such as GATA-2, cMyb, Growth factor independent 1 (Gfi-1), and TFs of

the HOX family, are involved in HSC self-renewal, differentiation, and maintenance of quiescence [38].

Maintaining HSC quiescence is of crucial importance not only for sustaining the HSC pool during hematopoiesis but also for reducing the accumulation of damaging mutations that could lead to hematologic disorders [45].

1.3 Disorders of the blood system

Blood disorders refer to any condition that impairs the function of one or more components of the blood. Generally, hematologic disorders originate from deviations from normal hematopoiesis. As previously discussed, the hematopoietic system needs to be highly dynamic in order to sustain the high turnover rate of mature blood cells, and this makes HSPCs susceptible to mutations that can lead to diseases, such as blood cancer [52].

1.3.1 The blood system is sensitive to the development of diseases

Somatic mutations accumulate in HSPCs over time, and in humans, each HSPC gain about one somatic mutation per decade [53]. Thus, aging is associated with an increased mutational burden in HSPCs. As mutations accumulate and combine in the cells, various HSPCs possessing distinct genetic patterns are made over time. The majority of the mutations are insignificant regarding the function of the cell; however, some might provide a fitness advantage [54]. HSPCs possessing such mutations could have an increased proliferation rate and form colonies that produce a significant number of abnormal blood cells. This process, referred to as clonal hematopoiesis, can in some cases lead to the development of blood cancer and other blood disorders related to age [52].

Mutated genes responsible for clonal hematopoiesis are termed driver genes, and in most cases of clonal hematopoiesis, there is only one driver gene mutation. However, in cases where clonal hematopoiesis results in malignancy, several driver gene mutations accumulate [53]. Clonal hematopoiesis of indeterminate potential (CHIP) refers to clonal

mutations associated with cancer that are present in more than 4% of the peripheral blood (PB) cells of individuals without any hematologic malignancy [55]. However, it has been shown that the presence of CHIP is associated with increased risks of developing hematologic malignancy [56]. This may occur if the initial CHIP driver mutation cooperates with additionally acquired driver mutations [52]. In a study by Welch et al., it was demonstrated that cooperative mutations on top of CHIP could lead to acute myeloid leukemia (AML) [53].

1.3.2 Acute myeloid leukemia

Leukemia is a type of blood cancer characterized by a large number of abnormal and immature white blood cells present in the hematopoietic niches and in the PB [57]. Leukemia is caused by genetic mutations in HSCs and HPCs, which results in deregulated hematopoiesis. The leukemic cells respond abnormally to cell cycle regulation and apoptotic signals, leading to disruption of normal differentiation. Hence, the leukemic bulk cells, or blast cells, fail to differentiate into fully mature blood cells, leading to disease [58]. Leukemic symptoms are nonspecific but may include fatigue, bleeding, weight loss, and fever. Leukemia can be found both in lymphoid and myeloid lineages, allowing subdivision of leukemia into lymphoid leukemia and myeloid leukemia, respectively. The disease can further be divided into acute and chronic leukemia based on how fast the blast cells develops [59].

AML is the most common form of leukemia, and it accounts for 80 percent of acute leukemia in adults [59]. In the United States, the annual incidence of the disease is about 2.4 per 100 000 individuals, increasing to 12.6 per 100 000 for people over 65 years of age [60]. Despite extensive research and improved understanding of AML biology, AML is still a challenging disease to treat due to its great heterogeneity. Today, less than 40% of adult AML patients under 60 years of age are cured, and only 5-15% of older patients are cured [57].

AML is a heterogeneous disease where myeloid blast cells infiltrate the BM, the PB, and other tissues through clonal hematopoiesis [57]. Extensive genetic techniques allowing

the identification of chromosomal abnormalities, as well as small genetic mutations, have unveiled a landscape of AML-associated mutations and karyotypic abnormalities [57]. Combined with genetic mutations derived from clonal hematopoiesis, these compose the great heterogeneity in the mutational pattern exhibited by AML patients, which makes the disease difficult to treat [61]. Today, the standard treatment for young and fit AML patients is intensive chemotherapy followed by allogeneic stem cell transplantation [62], whereas elderly and unfit AML patients are treated with palliative low-intensity regimes or best-supportive care [63].

1.4 Application of hematopoietic stem cells for treating blood disorders

Operationally, HSCs are defined by their capacity to hierarchically reconstitute the entire blood system of a recipient [1]. HSC transplantation refers to the use of HSCs from any donor aiming to colonize the marrow of a recipient, replacing or partly replacing the recipient's hematopoietic system [64]. Today, BM transplantation is used to treat a variety of blood disorders, such as leukemia, congenital metabolic defects, hemoglobinopathies, and lymphoma [65]. Generally, there are two main types of stem cell transplants: autologous and allogenic. Autologous stem cell transplants are harvested form the patients own body, whereas allogeneic stem cell transplants are taken from another person, a healthy donor [66]. In 2016, 8000 allogeneic BM transplantations were reported in The United States to the Center for International Blood and Marrow Transplant Research (CIBMTR), and even a higher number of autologous transplantations were performed [67]. Preparing patients for BM transplantation includes making space for the donor HSCs in the recipient BM. Depending on the disease, this can be performed by irradiation, or by the use of cytotoxic drugs [1] which is the strategy performed before stem cells are transplanted to AML patients [68].

1.4.1 Acute myeloid leukemia - therapeutics

The standard treatment strategy for AML patients can be subdivided into induction therapy and consolidation therapy. The induction therapy aims to reach complete remission (CR) (maximum reduction) of leukemic cells. This is carried out by chemotherapy [68].

Following CR, consolidation therapy aims to prevent relapse and eliminate minimal residual leukemic cells in the BM. Generally, consolidation therapy comprises two different strategies: additional chemotherapy and allogeneic or autologous HSCs transplantation (ASCT). These can either be used alone, or they can be combined [62]. Depending on the patient's disease prognosis, overall health, and the availability of a stem cell donor, the most suitable form of consolidation therapy is carried out. Generally, AML patients with low risk genetics have a good prognosis and will normally receive additional chemotherapy, whereas, patients with intermediate or high-risk genetics, will proceed with stem cell transplantation [61].

1.4.2 Clinical potential of hematopoietic stem cells upon transplantation

Evidence demonstrating curative BM transplantation of lethally irradiated mice [69] and leukemic mice [70], as well as improved understanding of the human leukocyte antigen (HLA) system brought about the first successive BM transplantation in human patients in the 1960s, with long-term survival [71]. Since then, further therapeutic improvements have been accomplished. Today, HSCs can be collected from core blood (CB) or PB after treatment with cytokines to mobilize the stem cells. This approach is less invasive compared to harvesting BM cells by multiple aspirations from donors [72]. Moreover, donors for allogeneic transplantation can be picked from donor registries worldwide, and side effects (e.g., infections) resulting from the transplantation procedure are better controlled [73]. Hence, BM transplantation have become a standard treatment procedure, and it is currently used to treat a variety of malignant and non-malignant hematologic disorders [74].

The HLA system is a complex of human genes encoding cell surface proteins involved in regulating the immune system [75]. Upon allogeneic HSC transplantation, a donor is matched based on the patient's HLA system. However, small immunological changes might be present between the transplanted cells and the recipient cells, leading to donor T cells recognizing recipient antigens. If this is the case, the donor T cells will attack the recipient cells, leading to so-called graft-versus-host-disease (GvHD) and/or a graft-versus-leukemia (GvL) effect in leukemic patients [71]. The symptoms of GvHD vary

from mild to more severe, and despite progress in understanding the biology of the disease, it has been found complicated to treat [76]. In contrast, it has been demonstrated that patients undergoing allogeneic HSC transplantation benefit from the GvL effect, where donor T cells contribute to eradicate residual AML cells [77]. Patients receiving autologous stem cell transplants do not benefit form the GvL effect, however, the risk of developing GvHD upon ASCT transplantation is eliminated and there is no need for HLA-matched donors. Moreover, comparing ASCT to allogeneic stem cell transplantation, ASCT is associated with lower rates of nonrelapse mortality and graft failure. In addition, ASCT is not followed by the need of long-term immunosuppression, and the development of infections. However, when collecting patient stem cells for ASCT, there is a risk for cancer cell contamination in the autograft, which upon transplantation could lead to relapse [78].

Hematopoietic tissues exhibit low frequencies of HSCs, and the absence of markers unique to HSCs makes it complicated to isolate them with sufficient purity and yield for transplantation [79]. Today, positive surface expression of the glycoprotein, CD34, is routinely used in the clinic as a marker for HSCs [80]. However, CD34 is not only expressed by HSCs, but also by lineage-committed HPC, such as GMPs. This results in great heterogeneity in the sorted HSCs population, even though CD34 is used in combination with other surface antigens. Additionally, CD34 is expressed by several AML cancer cells which limits its use upon preparing autologous stem cell transplants for AML patients [81]. Therefore, further characterization of the HSC immunophenotype is required to improve our understanding of HSC biology and current strategies for assessment of HSC numbers in HSC grafts and preparation of HSC grafts.

1.5 Endomucin

In study, Matsubara et al., showed that Endomucin (EMCN) is highly expressed on murine BM HSCs and progenitor cells and that the $EMCN^{+}CD34^{-}$LSK population is enriched for LT-HSCs. In the YS, they also found that EMCN expression could separate multilineage embryonic hematopoietic cells from committed erythroid progenitors. Further, it was demonstrated that developing HSCs in the AGM were enriched in hematopoi-

etic cell populations expressing EMCN. These findings confirmed that EMCN is expressed throughout development [82]. In a study by Reckzeh and other colleagues at the Finsen lab, *EMCN* was also defined as a marker for human HSCs. Importantly this study demonstrated $Lin^{-}EMCN^{high}$ BM cells were significantly enriched for immunophenotypic HSCs compared to $Lin^{-}EMCN^{low}$ BM cells. Additionally, they demonstrated that only the $Lin^{-}EMCN^{high}$ population had the capacity for human long-term multilineage engraftment, in contrast to the $Lin^{-}EMCN^{low}$ BM cells [83]. These findings suggests EMCN as a novel LT-HSC surface marker both for mice and for humans. Additionally, it has been reported that while EMCN is highly expressed on murine and human HSCs, its expression gradually declines as the cells differentiate via MPPs to lineage-committed HPSs. MPPs express moderate levels of EMCN, while more differentiated progenitors, such as GMPs, do not express the protein [81].

1.5.1 Endomucin structure and expression

EMCN is a type I integral membrane O-sialoglycoprotein closely related to the CD34 surface marker widely used as a HSC marker in the clinic [84]. EMCN expression was originally identified on murine and human endothelial cells (EC) [85], and its expression in murine and human HSCs was confirmed later [82], [83]. The extracellular domain of EMCN contains serine and threonine residues which are heavily O-glycosylated. This contributes to the rigid and lengthened structure seen in the protein, which is important for its ability to regulate cell-cell and cell-matrix signaling [86].

1.5.2 Function in endothelial cells

EMCN is expressed luminally on the endothelium surface in venules and in capillaries; however, it is not expressed on arterial endothelium [84]. In ECs, it has been shown that EMCN is involved in the negative regulation of adhesion to other cells. A study by Ueno et al. suggests that during development, EMCN is essential for the detachment of HSCs from endothelium [87]. Furthermore, it has been demonstrated that EMCN expressed on ECs prevents the binding of blood leukocytes, lowering inflammatory responses in non-inflamed tissues [86]. EMCN counteracts inflammatory cytokines that promote the adhesion of inflammatory cells. However, during inflammation, inflammatory cytokines

will down-regulate the EMCN expression on the ECs, allowing proper response [88]. Moreover, it has been shown that knock-down of *Emcn* results in impaired angiogenesis, suggesting that the protein also plays an essential part in the formation of new blood vessels [89].

1.5.3 Function in hematopoiesis

At present, the function of EMCN in HSCs has not yet been identified. However, in a study by Holmfeldt et al., EMCN was identified as one of 17 new regulators of HSPC repopulation following transplantation. The study also demonstrated that *Emcn* knock-down results in loss of function in terms of HSC repopulation. [90]. Also, on the EMCN intracellular domain, three potential Phosphokinase C (PKC) phosphorylation sites have been identified, suggesting that the protein might be important for signaling in hematopoiesis [87]. Despite this discovery, no down-stream signaling pathways have to the best of our knowledge been identified for EMCN.

1.5.4 EMCN in cancer

To date, the expression pattern and function of EMCN in cancer show great variance depending on the cancer type. In a study performed by Sung and colleagues, it was demonstrated that EMCN expression is downregulated in primary central nervous system lymphoma [91], while Dai1 et al., showed that high expression of EMCN in stomach adenocarcinoma is associated with high mortality [92]. It has been shown that EMCN expression in gastric cancer correlated positively with peritoneal metastasis and oncogenesis [92], [93]. However, it has been demonstrated that EMCN is not or lowly expressed in hematopoietic malignancies, such as in AML [81].

2 Rationale of the study

Since somatic mutations accumulate in the HSCs over time, the blood system is sensitive to the development of blood cancer and other hematopoietic disorders related to age [52]. HSCs have the capacity to reconstitute the entire blood system of recipients after blood loss or injury [1], and today allogeneic HSCs transplantation is used to treat a variety of blood disorders, such as AML [78] [62]. Therefore, more sophisticated marker combinations are needed to further refine the immunophenotype of HSCs. The latter will allow for the sorting of more pure HSC populations to improve our understanding of stem cell biology. In addition, this will also allow for a better assessment of the HSC capacity of HSC grafts, to avoid potential graft failure in the clinical setting.

Today, the HSC surface marker, CD34, is used as a marker for the assessment of HSCs in allogeneic HSC grafts [80]. However, CD34 also is expressed by lineage-committed HPCs, resulting in high heterogeneity in the HSC population isolated upon transplantation. Additionally, CD34 is expressed by several AML cancer cells (Figure 4A), which limits its use for sorting tumor-free HSC cell grafts from AML patients applicable for autologous HSC transplantation [81].

It has been reported that EMCN is highly expressed on the surface of murine and human HSCs, and that it enriches for immunophenotypic HSCs [82] [83]. In addition, it has been demonstrated that EMCN expression declines as the cells differentiate via MPPs to HPCs. Based on these findings, EMCN appears to be a promising new HSC marker. Moreover, EMCN is not expressed by AML cancer cells (Figure 4B), and can therefore be used to purify tumor-free HSC grafts from AML patients for autologous transplantation [81]. This might be alternative consolidation treatment if allogeneic donors are lacking, or if the toxicity of allogeneic HSC transplantation is considered to high.

The aim of this project was to explore the function of EMCN expressed by murine LT-HSCs using a novel *Emcn* conditional knock-out (KO) model.

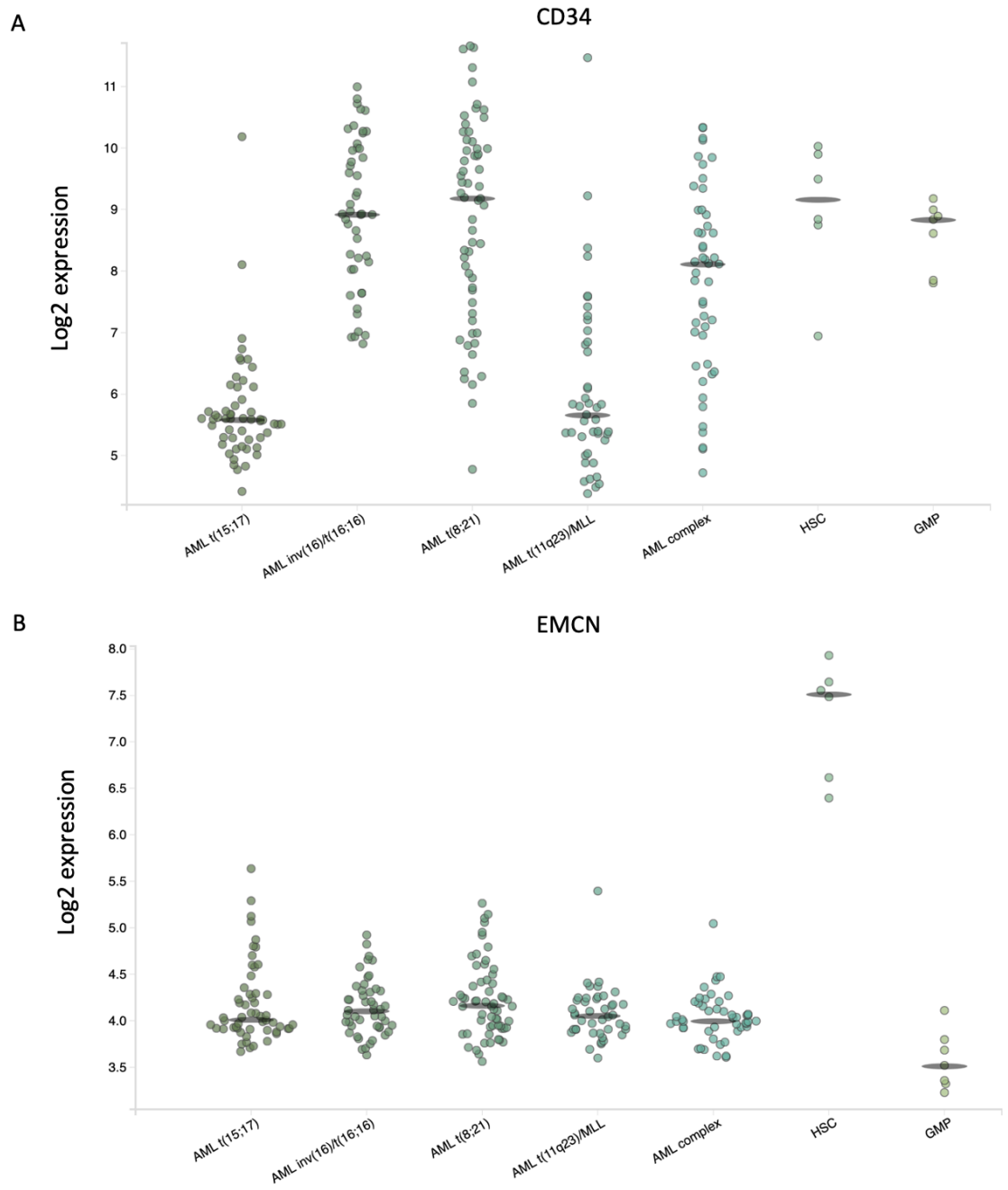

Figure 4: **The expression level of CD34 and EMCN in AML cancer cells and normal HSCs and GMPs** The levels of mRNA expression in AML t(15;17), AML inv(16)/t(16;16), AML t(8;21), AML t(11q23)/MLL, AML complex karyotype, normal HSCs, and normal GMPs is presented on a Log2 scale. The circle demonstrates the average level of expression.**(A)** CD34 is highly expressed by AML inv(16)/t(16;16), AML t(8;21), and AML complex karyotype, as well as by normal HSCs and normal GMPs. AML t(15;17) and AML t(11q23)/MLL cells exhibit low CD34 expression. **(B)** AML cancer cell and normal GMPs express low levels of EMCN transcripts, while HSCs express high levels. Figure from Bagger et al. [81].

3 Materials and methods

3.1 Materials

3.1.1 Mice

The *Emcn* conditional KO model was obtained from in-house breeding at the core facility for transgenic mice, University of Copenhagen. B6.SJL females were also obtained from in-house breeding. The C57BL/6 mice were purchased from Taconic (Denmark).

3.1.2 Antibodies

Table 1: **Anti-mouse antibodies for cell analysis and sorting on FACS**

Antigen	**Flurochrome**	**Manufacturer**	**Catalog number**	**Clone**
CD45.1	APC	Biolegend	110714	A20
CD45.2	FITC	Biolegend	109806	104
B220	Alexa Fluor 700	Biolegend	103232	RA3-6B2
CD3e	PE	Biolegend	100308	145-2C11
CD11b	PE-Cyanine7	eBioscience	25-0112-82	M1/70
Gr1	PE-Cyanine7	Biolegend	108416	RB6-8C5
EMCN	PE	eBioscience	12-5851-82	V.7C7
CD16/32	Alexa Fluor 700	eBioscience	56-0161-82	93
CD11b	PE-Cyanine5	Biolegend	101212	M1/70
GR-1	PE-Cyanine5	Biolegend	108410	RB6-8C5
CD3e	PE-Cyanine5	eBioscience	15-0031-82	1452C11
Ter119	PE-Cyanine5	Biolegend	116210	TER-199
B220	PE-Cyanine5	Biolegend	103210	RA3-6B2
CD48	PE-Cyanine7	Biolegend	103424	145-2C11
cKit	APC-eFluor 780	eBioscience	47-1171-82	2B8
CD150	Brilliant Violet 650	Biolegend	115932	TC15-12F12.2
Sca-1	Pacific Blue	Biolegend	108120	D7
CD150	Brilliant Violet 711	Biolegend	115941	TC15-12F12.2
Sca-1	APC	Biolegend	108112	D7
CD45	APC	Biolegend	103112	30-F11
Ki67	FITC	eBioscience	11-5698-82	SolA15

3.1.3 Primers

Table 2: **Primers used for genotyping**

Target	**Sequence**	**Manufacturer**
Emcn floxed-F	CCCTTTCTCAAGAAGGGTCTCT	Eurofins Genomics, Denmark
Emcn floxed-R	TCCCTTCAGTGGAAACGAACT	Eurofins Genomics, Denmark
Cre-F	GCC TGC ATT ACC GGT CGA TGC AAC GA	Eurofins Genomics, Denmark
Cre-R	GTG GCA GAT GGC GCG GCA ACA CCA TT	Eurofins Genomics, Denmark

Table 3: **Primers used for RT-qPCR**

Target	**Sequence**	**Manufacturer**
Emcn-F	AAGTAGGAATGGGCAGCGTC	Eurofins Genomics, Denmark
Emcn-R	TCTGAACATCTTTGCCGTCCT	Eurofins Genomics, Denmark
Hprt -F	GGTTAAGCAGTACAAGCCCCA	Eurofins Genomics, Denmark
Hprt -R	TCCAACAAAGTCTGGCCTGT	Eurofins Genomics, Denmark

3.1.4 Kits

Table 4: **Kits**

Kit	**Manufacturer**	**Catalog number**
RNeasy Plus Micro Kit	Qiagen	74034
iScript cDNA Synthesis Kit	Bio-rad	1708891
Lineage Cell Depletion Kit	Miltenyi Biotec	130-090-858
Flow Cytometry Assay Kit	Invitrogen	C10646

3.1.5 Consumables

Table 5: **Consumables**

Product	**Manufacturer**	**Catalog number**
BD Pharm Lyse lysisng buffer	BD Biosciences (NJ, USA)	555899
Fetal Bovine Serum (FCS)	Gibco/ThermoScientific	16250078
Chelex 100 Chelating Resin	Bio-Rad	1432832
Tween 20	Fisher Scientific	BP337500
Proteinase K	Sigma-Aldrich	3115828001
DreamTaq Green PCR Master Mix	ThermoFisher	K1081
UltraPure Agarose	ThermoFischer	16500-100
GelRed	Biotium Inc.	41003
Tris-borate-EDTA (TBE)	Alfa Aesar	J62449
100bp DNA ladder	New England Biolabs (NEB)	NEB-N3231L
OneComp eBeads	Invitrogen	01-1111-42
Poly(I)-Poly(C)	GE Healthcare	27-4732-01
7AAD	Invitrogen	A1310
Ethanol	Sigma-Aldrich	109-56-8
Solution 13	Chemometec	910-3013
Isaderm Vet.	Dechra Veterinary Products	7046264437896
PFA	SigmaAldrich	F8775
DAPI	Merck	10236276001
Phosphate-buffered saline (PBS)	Made in the lab	
0,2mL tube and cap strips	Thermo Fischer	AB-0490
3mL Luer-lok tip syringe	BD Biosciences	309658
50μm Cup Filcons	BD Biosciences	340632
70μm nylon cell strainer	Falcon	352350
Microvette 500 K3E	Sarstedt, Germany	20.1341.100
LightCycler 480 Multiwell Plate 96	Roche Diagnostics	04729692001

PBS was made in the lab - composition shown in Appendix 1.

3.1.6 Equipment

Table 6: **Equipment**

Product	**Use**	**Manufacturer**
Centrifuge 5417R	Centrifuge for Eppendorf tubes	Eppendorf
MS2 Minishaker	Vortexer	IKA
4-16S centrifuge	Spin out centrifuge	Sigma
C1301R-230V	Mini centrifuge	Labnet
LSRFortessa^{TM} cell analyser	FACS	BD Biosciences
FACSAria^{TM}	FACS	BD Biosciences
NucleoCounter NC-3000	Cell count	Chemometec
DS-11 FX Spectrophotometer	RNA/DNA concentration	DeNovix
ThermoCycler T100	PCR	Biorad, Germany
Gel Doc XR+ Gel Documentation System	Visualize DNA fragments on gel	Bio-Rad
Faxitron CP160	X-ray irradiation	Faxitron X-Ray Corp. IL, USA
Element HT5	Animal Bloodcounter	Heska
Lightcycler480	qPCR	Roche Diagnostics
Veriti thermal cycler	cDNA synthesis	Applied Biosystems

3.2 Methods

All antibodies (Table 1), primers (Table 2 and Table 3), kits (Table 4), consumables (Table 5), and equipment (Table 6) used in the experiments are shown in section 3.1 Materials.

3.2.1 Mice

All mice were maintained in accordance with the Danish animal guidelines, and research conducted with the mice was approved by the Danish Animal Ethical Committee. Mice were kept at 22°C in a 12h light-dark cycle in individually ventilated cages under specific pathogen-free conditions. The water and the ad libitum diet fed to the mice were autoclaved. Both males and females were used in the experiments in which age- and gender-matched littermates served as controls.

3.2.2 Generation of the *Emcn* conditional knock-out mouse model

A novel knock-out strategy, called conditional mutagenesis, was developed in 1994, permitting the study of the effects of gene knock-out (KO) only in specific cell types and/or at specific time points [94]. Conditional KO models contain recombinase recognition (LoxP)

sites flanking (or floxing) the gene of interest, and a DNA recombinase, Cre, that recognizes these sites. Upon Cre activation, the two LoxP sites will be recombined, resulting in a reciprocal exchange of DNA strands between the sites. If the LoxP sites are oriented in the same direction on linear DNA, this will lead to gene KO. Several promotors for Cre activation have been used in conditional KO models; however, the most commonly used in experimental hematology is the interferon-inducible promotor Mx1 [95]. The inducable promotor allow for temporally control of Cre recombinase expression which further allow the knock-out to be activated at a desired time-point, only in somatic cells [96]. Conditional KO mice are generated by crossing transgenic Cre mice with mice carrying homozygous conditional alleles [97].

The insertion of LoxP sites within *Emcn*

The *Emcn* conditional KO model was generated by the core facility for transgenic mice using the CRISPR/Cas9 technology to insert LoxP sites on either side of exon 1 of the *Emcn* gene. Exon 1 was chosen as the target because deletion of the first ATG codon in exon 1 was believed to knock out EMCN, it is shared by all transcripts coding EMCN, and the size of exon 1 is well suited to the targeting strategy. The floxing of exon 1 was initiated by introducing CRISPR-associated protein 9 (Cas9) administrated double-stranded breaks on either side of the exon, followed by the induction of a homology-directed repair cassette containing the LoxP-Exon1-LoxP sequence. Precise integration of the LoxP sites, which were both orientated in 5' to 3' direction, was ensured by the repair templates homology to the sequences alongside the insert location. The targeting strategy is illustrated in Figure 5. Successful insertion of the repair template into mouse embryonic stem cells (mESCs), transfected with gRNA and the template, was confirmed by genotyping. These stem cells were then microinjected into morula stage C57BL6/N embryos, which were transferred into pseudopregnant recipient mice. The resulting offspring were screened for chimerism. Since the cells originated from the C57Bl6/N embryos and those inserted with the floxed sequence contributed to two different fur colors, this screening could easily be carried out. Mice with the highest chimerism were crossed so that all offspring carried the floxed sequence. When the mice were 2-3 months, sperm was collected from the F0 males, and embryos were made by in vitro fertilization of oocytes from Mx1Cre mice (Cre on only one allele) and floxed sperm cells. Pseudopregnant recipients

gave birth to the F1 pups in the in-house animal facility.

.

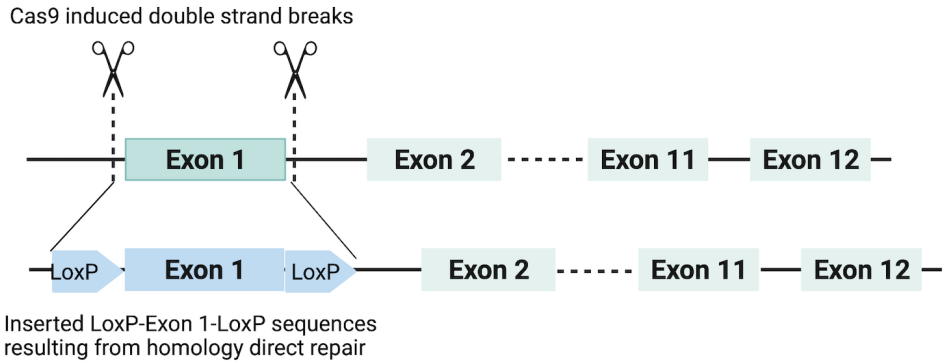

Figure 5: **Schematic illustration of the *Emcn* LoxP targeting strategy.** The scissors illustrate the cut sites, administered by gRNA and Cas9 nuclease, where the LoxP sites were introduced. Created with Biorender.

Breeding mice

All F1 mice had one floxed allele and one WT allele for *Emcn* ($Emcn^{fl/WT}$), and 50% of the mice were Mx1Cre positive. At the animal facility, the Mx1Cre positive F1 mice where bred with Mx1Cre negative F1 mice generating $Emcn^{fl/fl}$;Mx1Cre mice, $Emcn^{fl/fl}$ mice, $Emcn^{fl/WT}$;Mx1Cre mice, and $Emcn^{fl/WT}$ mice. Ear biopsies were taken by the animal facility to genotype these mice. Based on genotype, new breeding pairs were set up, preferentially crossing $Emcn^{fl/fl}$;Mx1Cre mice with $Emcn^{fl/fl}$ mice to generate mice exhibiting such genotypes for further breeding and for research. However, $Emcn^{fl/WT}$ mice were also used in some breeding pairs. The inheritance pattern for the Cre allele, as well as for the genetic variants of *Emcn* follow Mendelian inheritance. The inheritance pattern for the *Emcn* variants are exemplified in Figure 6.

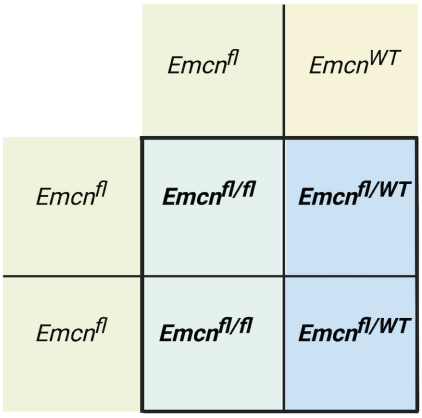

Figure 6: **Punnett square diagram.** The diagram shows how genetic variants of *Emcn* in mice are passed on to offspring following Mendelian inheritance. Green/yellow: parental alleles. Light blue/blue: possible combinations of parental alleles in offspring and its theoretical distribution. Created with Biorender.

3.2.3 Isolation of DNA from mouse biopsies

To genotype the mice, DNA was extracted from ear biopsies while the mice were alive and from whole BM (WBM) cells after death to verify the genotype. DNA extraction was carried out by mixing the biopsies with the master mix shown in Table 7. The Chelex stock and the Proteinase K disintegrate the biopsy tissue to access the DNA. The Chelex stock contains beads that, upon shaking, disrupt the membrane of the cells. Proteinase K digests the proteins. The samples were incubated at 55°C on shakers, 1150 rmp for three hours. This was followed by heat-inactivation at 70°C, for 10 minutes. The samples were then vortexed and centrifuged at 13.000 g for 15 minutes. Next, the supernatant containing the DNA was transferred to fresh 1.5 Eppendorf tubes and stored at 4°C until further use.

Table 7: **Master mix for DNA extraction.**

	Amount per sample
Chelex stock	200 μL
Tween20 (10%)	2 μL
Proteinase K	2 μL

3.2.4 Genotyping mice

Two separate polymerase chain reactions (PCR) were performed to identify floxed (and WT) *Emcn* (reaction 1), and the presence/absence of Cre (reaction 2) in the mice. The PCR reactions were set up according to Table 8. The PCR master mix contained deoxynucleotide triphosphates (dNTPs), DreamTaq DNA Polymerase, green loading dye for gel electrophoresis, and $MgCl_2$ for enhancing the polymerase activity. The specific primers added to the reactions are shown in Table 2. The PCR reactions were run in a ThermoCycler T100 with thermal cycling allowing amplification of the target sequences. The annealing temperatures were specific for each set of primers. Table 9 and Table 10 shows the PCR temperature programs for *Emcn* and Cre, respectively. To study the PCR amplification of Cre and floxed *Emcn*, 10 μL of the PCR products were directly loaded on a 1.5 % and 2% TBE-buffer(0.5%) based agarose gel, respectively. 5 μL of a 100 base pair ladder (N3231) was also loaded, in addition to a positive and a negative control. PCR products from Cre positive mice and $Emcn^{fl/WT}$ mice (that were previously genotyped) were used as the positive controls. To be able to visualize the DNA bands on the gel, Gelred 1:20.000 was added to the TBE-buffer (0.5%) when the gel was made. The gel was placed in a chamber filled with TBE-buffer (0.5%) where an electrical current was separating the DNA fragments based on size. The gel electrophoresis was carried out at 180 volts for 45 minutes (Cre) and 3 hours (*Emcn*) before the DNA bands were visualized under UV light using the BioRad Gel Doc XR Imaging system.

Table 8: **Master mixes for the PCR reactions**

	***Emcn*^{fl} (reaction 1)**	**Mx1Cre (reaction 2)**
DreamTaq Green PCR Master Mix (2x)	10 μL	10 μL
Primer forward	1 μL	1 μL
Primer reverse	1 μL	1 μL
ddH_2O	7 μL	7 μL

Table 9: **PCR temperature program for *Emcn* - 35 cycles**

Step	**Temperature (°C)**	**Time**
Initial denaturation	94	5’
Denaturation	94	30”
Annealing	60	45”
Elongation	72	60”
Final elongation	72	5’

Table 10: **PCR temperature program for Cre - 35 cycles**

Step	**Temperature (°C)**	**Time**
Initial denaturation	94	2’
Denaturation	94	60”
Annealing	67	90”
Elongation	72	60”
Final elongation	72	5’

3.2.5 pI:pC treatment

The Cre recombinase in the transgenic Mx1Cre mice is controlled by the type I interferon (IFN) inducible Mx1 promoter [98]. Mx1 is inactive in healthy mice but is transcribed at high levels by administration of IFNs or synthetic double-stranded RNA, such as polyinosinic-polycytidylic acid (polyI:C). PolyI:C induces IFN production in murine interferon-responsive cells, including HSCs. Upon treating Mx1Cre positive conditional KO mice with polyI:C, the Mx1 promotes Cre expression, which can lead to induction of the knock-out [97].

To study the effect of EMCN knock-out in HSCs, $Emcn^{fl/fl}$;Mx1Cre mice and $Emcn^{fl/fl}$ mice (the latter serving as controls) were treated four times with 100 μL polyI:C. The polyI:C was introduced to the mice through intraperitoneal injection, carried out every second day. The injection site (right or left side of the stomach) was changed each time. To deliver the polyI:C, 3 mL syringes and 26G needles were used.

3.2.6 Tissue isolation and preparation

Washing was performed by adding 1 mL PBS/3%FCS followed by 5 minutes centrifugation at 300 g, if not otherwise stated.

Peripheral blood

To study blood composition in the mice, PB was collected. Blood was taken by facial vein puncture and collected into microvette 500 K3E tubes. This was performed by colleagues in the animal facility.

The PB was analyzed on an animal blood counter. The remaining blood was prepared

for antibody staining and FACS analysis. This was performed by lysis of erythrocytes carried out by mixing 100 μL blood (containing approximately 10x10^6 cells) with 1 mL 1x BD Pharm Lyse lysing buffer. Following a 15 minutes incubation step at room temperature (RT), the suspension was centrifuged at 300 g for 5 minutes. The supernatant was discarded, and the pellet was washed. Finally, the pellet was re-suspended in 200 μL PBS/3%FCS and kept on ice before the cells were stained with antibodies for flow cytometry analysis.

Bone marrow cells

To study BM composition in the mice and to isolate HSCs for transplantation, mice were sacrificed by cervical dislocation and cut open before femurs, iliac, and tibiae bones were collected. To prepare the BM cells for antibody staining, the bones were crushed in a mortar and the BM cells re-suspended in 10 mL PBS/3%FCS. The BM suspension was filtered through a 70 μm cell strainer to obtain single-cell suspensions. 100 μL of the cell suspension was taken out and diluted to a 1:10 ratio with PBS/3%FCS for cell counting. 5 μL Solution 13 was added to each sample in order to quantify cell concentration and viability upon counting the cells on a NucleoCounter.

In order to perform flow cytometry analysis of HSPC and to sort of HSCs, the BM cells had to be depleted of lineage-positive cells. This was performed using a Lineage Cell Depletion Kit and carried out following the manufacturer's instructions. Cell suspensions containing the desired number of WBM cells or lineage depleted cells (depending on the analysis) were centrifuged at 300 g for 5 minutes and re-suspended in 200 μL PBS/3%FCS prior to antibody staining for FACS analysis and cell sorting.

3.2.7 Flow cytometry and cell sorting

Prior to FACS analysis and sorting, PB cells and BM cells were stained with a combination of antibodies specific for cell surface markers expressed by unique cell types. Following staining with the antibodies, the cells were incubated for 30 minutes on ice. The cells were then washed to remove excess antibodies, before they were re-suspended in 400 μL (PB cells) and 700 μL (BM cells) PBS/3%FCS including 1:1000 Aminoactinomycin D

(7-AAD). The 7AAD was used for the discrimination of dead cells. Before the samples were analyzed/sorted by FACS, they were filtered through 50 μm cup filters.

Antibody staining and analysis of peripheral blood cells

Antibody staining of PB cells was carried out using a mixture of antibodies shown in the staining panel in Table 11. FACS analysis was then performed on the LSR Fortessa(BD).

Table 11: **Antibody staining panel for murine peripheral blood cells**

Antigen	**Flurochrome**	**Concentration mg/mL**	**Amount per blood sample (μL)**
CD45*	APC	0.5	0.8
CD45.1**	APC	0.5	0.8
CD45.2**	FITC	0.5	0.8
B220	Alexa Fluor 700	0.2	0.5
CD3e	PE	0.2	0.25
CD11b	PE-Cyanine7	0.2	0.2
Gr1	PE-Cyanine7	0.2	0.25

*Antibody used to stain PB cells 4 weeks after polyI:C treatment. ** Antibodies used to monitor the PB during transplantation assays.

Antibody staining and analysis of bone marrow cells

Analysis of mature BM cells was carried out by staining the WBM cells with the antibody mix shown in Table 12, followed by FACS analysis performed on the LSR Fortessa (BD). The analysis and sorting of HSCs were performed by staining with the antibody mixture shown in Table 13, followed by FACS analysis carried out on the BD FACS Aria III (BD).

Table 12: **Antibody staining panel for murine mature bone marrow cells**

Antigen	**Flurochrome**	**Concentration mg/mL**	**Amount per 10x10^6 cells (μL)**
*CD45	APC	0.5	1
**CD45.1	APC	0.5	1
**CD45.2	FITC	0.5	1
B220	Alexa Fluor 700	0.2	0.8
CD3e	PE	0.2	0.5
CD11b	PE-Cyanine7	0.2	0.25
Gr1	PE-Cyanine7	0.2	0.5

Table 13: **Antibody staining panel for murine hematopoietic stem cells**

Antigen	**Flurochrome**	**Concentration mg/mL**	**Amount per 10x10^6 cells (μL)**
*CD45	APC	0.5	0.8
**CD45.1	APC	0.5	0.8
**CD45.2	FITC	0.5	0.8
EMCN	PE	0.2	4
CD16/32	Alexa Fluor 700	0.2	4
CD11b	PE-Cyanine5	0.2	0.25
GR-1	PE-Cyanine5	0.2	0.5
CD3e	PE-Cyanine5	0.2	0.5
Ter119	PE-Cyanine5	0.2	0.5
B220	PE-Cyanine5	0.2	0.5
CD48	PE-Cyanine7	0.2	1
cKit	APC-eFluor 780	0.2	1
CD150	Brilliant Violet 650	0.2	2
Sca-1	APC	0.5	1

*Antibody used to stain BM cells upon analysis/sorting 4 weeks after polyI:C treatment. ** Antibodies used to stain BM cells at the end of transplantation assays (16w).

Cell cycle analysis

Incubation was performed for 30 minutes in RT and darkness, if not otherwise stated.

To study cell cycle state in HSCs, cell cycle analysis was performed on FACS following staining with DNA binding fluorescent dye (DAPI), and Ki-67 antibody conjugated to FITS. Simultaneous analysis of the nuclear proliferation-associated protein, Ki-67, and the quantity of cellular DNA allow for the distinction between cells in G_0, G_1, and S-G_2M phase [99].

Upon cell cycle analysis, BM cells were isolated, prepared, and lineage depleted as described above. 5x10^6 lineage depleted cells were then stained according to the antibody staining panel shown in Table 14. The cells were incubated with the antibody cocktail for 30 minutes on ice before the they were washed. This was followed by cell fixation and permeabilization, facilitating intracellular staining of the cells. The cells were re-suspended in 125 μL PBS/3%FCS before 125 μL PBS/4%PFA was added to fix the cells (performed in 4℃). Following incubation for 10 minutes, the cells were washed. To permeabilize the cells, they were re-suspended in 250 μL PBS/3%FCS containing 0.1%

saponin before they were incubated. Further, the cells were centrifuged for 5 minutes at 200 *g*, and the supernatant was discarded (about 50 μL supernatant was kept). 2 μL Ki67-FITC was then added prior to incubation for 30 minutes in RT. The cells were then washed and centrifuged for 5 minutes at 200 *g* before the cells were re-suspended in 150 μL DAPI staining solution (0.5 μg/mL) and incubated. Cell cycle analysis was performed on the LSR Fortessa (BD).

Table 14: **Antibody staining panel used for cell cycle analysis of HSCs**

Antigen	**Flurochrome**	**Concentration mg/mL**	**Amount per 10x10^6 cells (μL)**
EMCN	PE	0.2	4
CD16/32	Alexa Fluor 700	0.2	4
CD11b	PE-Cyanine5	0.2	0.25
GR-1	PE-Cyanine5	0.2	0.5
CD3e	PE-Cyanine5	0.2	0.5
Ter119	PE-Cyanine5	0.2	0.5
B220	PE-Cyanine5	0.2	0.5
CD48	PE-Cyanine7	0.2	1
cKit	APC-eFluor 780	0.2	1
CD150	Brilliant Violet 711	0.2	2
Sca-1	APC	0.5	1

Single stains and Fluorescence Minus One (FMO) controls

Upon preparations for FACS analysis and sorting, single stains were always made. These are essential because they reveal the level of spectral overlap between distinct fluorochromes enabling the removal or compensation for this overlap. Single stains were made by adding one drop of One Comp eBeads to 0.7 μL of antibody conjugated to fluorochromes. Single stains were made for all fluorochromes used in the assay. This was followed by 30 minutes of incubation on ice. Fluorescence Minus One (FMO) controls were also made prior to FACS analysis. FMOs are made by adding all fluorochromes used in the assay minus one, to samples of the same cells as those that are studied in the analysis. These were prepared parallel to, and in the same way as the cells that were stained for FACS analysis. FMOs are important in multi-color flow cytometry panels and assist in the determination of where to set the gates. Single stains and FMOs were used in this project to set the gates for positive and negative cell populations.

3.2.8 Transplantation assays

To date, HSC transplantation assays are the only functional assay that can prove whether a cell is a true long-term repopulating stem cell [1]. In order to investigate if LT-HSCs lose their "stemness" upon loss of EMCN, LT-HSC transplantation was performed. LT-HSC transplantation also allow the study of the cell-autonomous function of EMCN KO in WT BM microenvironment. The transplantation assays were carried out by transplanting cells (CD45.2) from polyI:C treated $Emcn^{fl/fl}$;Mx1Cre mice or $Emcn^{fl/fl}$ mice, from now on referred to as EMCN KO and EMCN WT mice, into lethally irradiated CD45.1 recipients (B6.SJL mice). The recipients were irradiated with an X-ray irradiator with a dose of 9 Gray (1 Gray/minute) to accomplish complete myeloablation. LT-HCSs from each donor mouse were transplanted into triplicates of recipients by tail vein injection using a 29G needle.

Long-term hematopoietic stem cell transplantation

4 weeks post polyI:C treatment, 200 EMCN KO or EMCN WT LT-HSCs (CD45.2) were transplanted together with 200.000 WBM support cells from a CD45.1 mouse into lethally irradiated recipients (CD45.1) (Figure 7). To prepare the transplant, 800 LT-HSCs (200 HSCs per recipient + extra) were sorted from each donor mouse on the BD FACS Aria III (BD). This cell suspension was mixed with 800.000 support cells that were calculated out from a single-cell suspension. PBS/3%FCS was added to a final concentration of 800 μL. 200 μL of the suspension was injected to each recipient mouse.

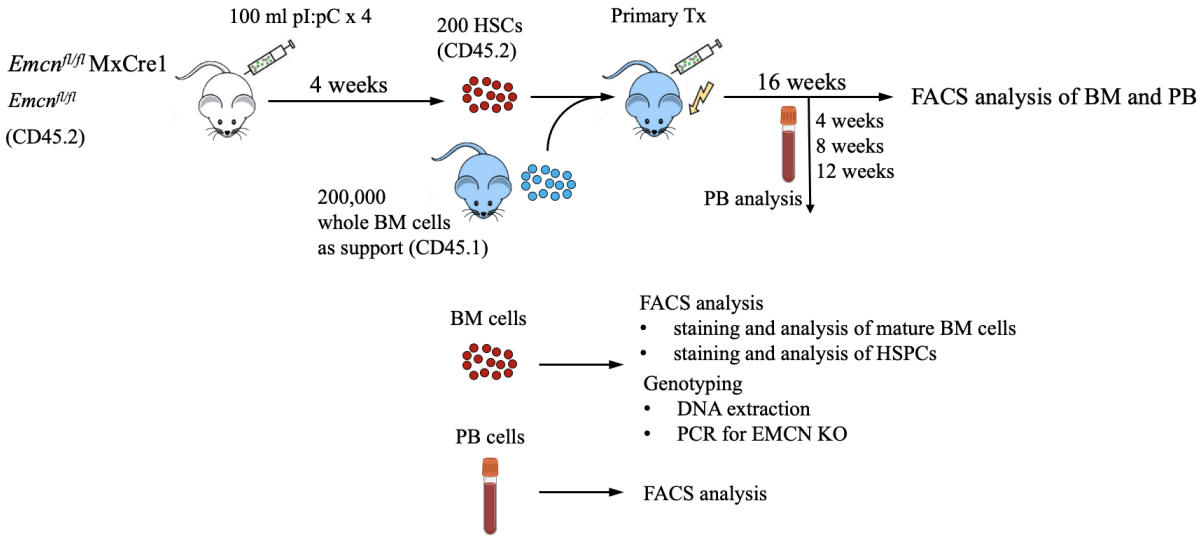

Figure 7: **Experimental set-up for the LT-HSC transplantation assay.** $Emcn^{fl/fl}$;Mx1Cre mice and $Emcn^{fl/fl}$ mice were treated with 4x100μL polyI:C. 4 weeks after the treatment, the mice were sacrificed and PB and BM were collected and analysed on FACS. BM cells were also used for genotyping. Using FACS, LT-HSCs were analysed and sorted out from the BM suspension upon transplantation. 200 LT-HSCs (CD45.2) from EMCN KO or EMCN WT mice were transplanted together with 200.000 WBM support cells (CD45.1) into lethally irradiated recipients (CD45.1). Blood composition in the recipients was monitored throughout the transplantation assay (at 4, 8, and 12 weeks time point), before BM and PB composition was studied at the end of the transplantation assay (16 weeks).

Competitive transplantation

To compare the re-populating capacity of EMCN KO LT-HSCs and EMCN WT LT-HSCs, a competitive transplantation assay was established. This was carried out by transplanting 250.000 WBM cells from $Emcn^{fl/fl}$;Mx1Cre mice or $Emcn^{fl/fl}$ mice, together with 250.000 WBM cells from a CD45.1 mouse, into lethally irradiated recipients (Figure 8). The intention was to treat the recipients with polyI:C following an adequate recovery period of 4 weeks. This was to study re-populating capacity of the donor HSCs while avoiding possible effects of the EMCN KO on the HSCs ability to home in the BM. However, the mice got lesions in their skin as a result of strong irradiation leading to termination of the competitive transplantation assay before the polyI:C treatment. Prior

to this, nails were cut twice a week to avoid itching, and the wounds were treated with Isaderm Vet., However, the mice had to me sacrificed due to substantial suffering.

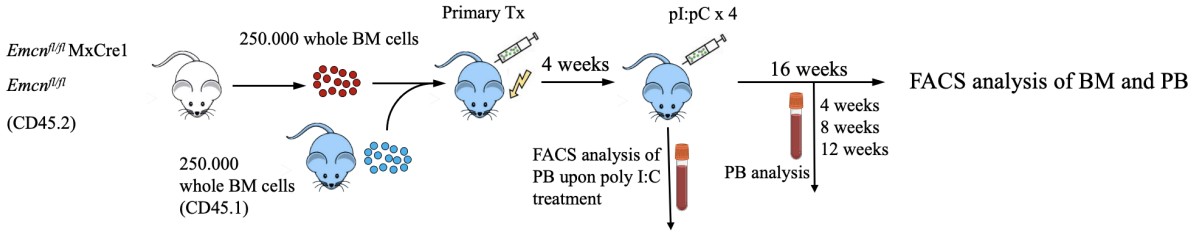

Figure 8: **Experimental set-up for the competitive transplantation assay.** 250.000 WBM cells (CD45.2) from $Emcn^{fl/fl}$;Mx1Cre mice or $Emcn^{fl/fl}$ mice were transplanted together with 250.000 WBM competitor cells (CD45.1) into lethally irradiated recipients (CD45.1). Following 4 weeks of recovery, the intention was to analyse PB using FACS, and to treatment the mice with 4x100μL polyI:C. During the transplantation assay, PB was supposed to be monitored by FACS analysis (at 4, 8, and 12 weeks), before BM and PB composition were analysed 16 weeks post transplantation.

3.2.9 Analysis of *Emcn* on the transcriptional level using RT-qPCR

To study the expression of *Emcn* on a transcriptional level in mice where LoxP sites were flanking exon 1, RT-qPCR was performed. C57BL/6 mice were used as controls. Using RNeasy Plus Micro Kit, RNA was isolated from WBM cells and LT-HSCs according to the manufacture's instructions. cDNA was then synthesized from the RNA using iScript cDNA Synthesis Kit following the protocol from the manufacturer. The cDNA concentration was measured using DS-11 FX Spectrophotometer. A primer master mix was prepared for each primer pair included in the experiment, according to table 15, using the primers presented in Table 3. Primers for the amplification of *Emcn* cDNA and *Hprt* cDNA was used. The primers used for the detection of *Emcn* expression was targeting exon 2. *Hprt* is a housekeeping gene and was used to normalize the general level of transcription in the samples. 15 uL of the relevant primer master mix was transferred to a lightcycler 96 well plate, before 5 uL cDNA containing 1-100 ng template were added to the the master mix. Triplicates were made for each cell type included in the experiment. The samples were run on Lightcycler qPCR machine.

ΔcT values representing *Emcn* transcript levels in $Emcn^{fl/fl}$ and C57BL/6 WBM cells and LT-HSCs were calculated by subtracting the mean cT value of *Hprt* from the mean cT value of *Emcn*.

Table 15: **Master mix qPCR**

Reactions	**Stock**	**Volume**
SYBR™ Green Master Mix	-	10 uL
Primer F	10 uM	1 uL
Primer R	10 uM	1 uL
H2O	-	To total volume
Total volume		**15 uL**

3.2.10 Statistical analysis

Flow cytometry data were analysed using FlowJo Software. For graphical representation of FACS data, RT-qPCR data, and blood count data, GraphPad Prism 9 software was used. Multiple comparisons were analysed using two-way ANOVA and grouped analysis. Pairwise comparison were performed using a Student's t-test. A p value < 0.05 was considered statistically significant. Data are presented as mean ± standard deviation (SD) or as mean ± standard error of mean (SEM).

4 Results

4.1 Induction of the conditional knock-out

4.1.1 *Emcn*$^{fl/fl}$;Mx1Cre mice and *Emcn*$^{fl/fl}$ mice were identified and selected based on genotyping

Following DNA extraction from ear biopsies, two different PCRs with primers directed towards *Emcn* and Cre were performed in order to identify *Emcn*$^{fl/fl}$;Mx1Cre mice and *Emcn*$^{fl/fl}$ mice that could be used for experiments. Samples amplified for *Emcn* were loaded on agarose gels to study if exon 1 was flanked with LoxP sites. Figure 9A show a representative gel that was used to identify *Emcn*$^{fl/fl}$ mice. DNA fragments of floxed *Emcn* constitute the DNA bands of 671 base pairs visible on the gel. Based on differences in base pair numbers, these bands could be distinguished from bands made up of wild type *Emcn*, constituting 603 base pairs. Mice exhibiting only the 671 bp band were considered homozygous for the *Emcn* floxed allele (see lane 2, 3, 7, 8, 10, and 11), while mice showing both the 671 and the 603 bp band were considered heterozygous (lane 4, 5, 6, and 9). In order to distinguish *Emcn*$^{fl/fl}$ mice where the EMCN KO could be induced, from those that would serve as controls in upcoming experiments, the presence/absence of Cre was investigated. The Cre could be identified by the presence of 705 bp bands on the gel loaded with the PCR products amplified for Cre. Figure 9B shows a representative gel used to study the presence of Cre in the mice. Based on the hypothesis that the EMCN expression in Cre positive (lane 4, 7, and 8) *Emcn*$^{fl/fl}$ mice would be knocked out upon polyI:C treatment, these mice were selected for experiments. Cre negative *Emcn*$^{fl/fl}$ mice was further used as controls.

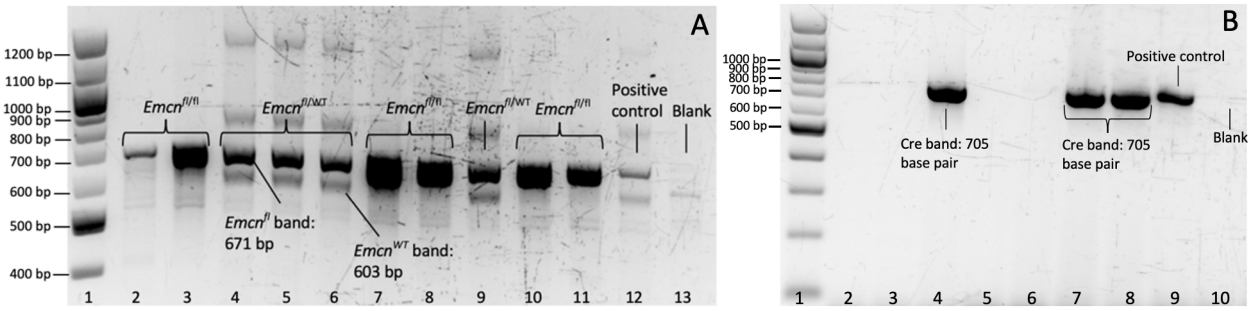

Figure 9: **Gels identifying *Emcn*$^{fl/fl}$;Mx1Cre mice and *Emcn*$^{fl/fl}$mice.** The 100 base pair ladder (N3231) was loaded in the first lines of the gels. **(A)** Representative gel for the identification of *Emcn*$^{fl/fl}$ mice. DNA fragments of floxed *Emcn* constitutes the 671 bp bands on the gel, whereas the 603 bp bands represents *Emcn*^{WT} DNA fragments. Lane 2, 3, 7, 8, 10, and 11 show only *Emcn*^{fl} bands, while lane 4, 5, 6, and 9 show bands both for *Emcn*^{fl} and *Emcn*^{WT}. Lane 12 represents the positive control showing the WT and the floxed *Emcn* band. Lane 13 shows the blank control. Unexpected bands of about 1200 and 900 bp can be seen in lane 4, 5, 6, 9, and 12. **(B)** Representative gel for the identification of Cre-positive mice. The 705 bp band present in lane 4, 7, and 8 is made up of Cre DNA. Line 9 show the Cre band of the positive control, whereas line 10 represent the blank control.

4.1.2 PolyI:C induce the knock-out of EMCN in *Emcn*$^{fl/fl}$;Mx1Cre mice

The *Emcn*$^{fl/fl}$;Mx1Cre mice and the *Emcn*$^{fl/fl}$ mice (controls) identified and selected based on genotyping were treated with polyI:C. This synthetic double-stranded RNA component promotes the expression of Cre recombinase by the activation of its Mx1 promotor [97]. This was performed to facilitate the recombination of the LoxP sites flanking *Emcn* exon 1 in the *Emcn*$^{fl/fl}$;Mx1Cre mice.

Two similar, but time separated, experiments were carried out during the project. In the first experiment, from now on referred to as exp. 1, 2 *Emcn*$^{fl/fl}$;Mx1Cre and 2 *Emcn*$^{fl/fl}$ mice were treated with polyI:C. In the second experiment, exp. 2, 6 mice of each genotype were treated; however, 1 *Emcn*$^{fl/fl}$;Mx1Cre mouse died during the treatment period. BM cells were isolated 4 weeks after the treatment when the mice were sacrificed upon the start of the transplantation assays. To investigate if the knock-out was

induced, genotyping was performed following DNA isolation from the BM cells. Knock-out of *Emcn* exon 1 could be identified by the presence of DNA bands of 302 bp on the gel loaded with the PCR products amplified for *Emcn*. Figure 10 shows a representative gel for the identification of the knock-out mice. In this gel, PCR products from polyI:C treated $Emcn^{fl/fl}$;Mx1Cre mice were loaded in lane 3, 4, and 9, exhibiting the 302 bp KO band. These lanes showed only this one band which indicated that EMCN was fully knocked out in the Mx1Cre positive mice following polyI:C treatment. This result was representative for all $Emcn^{fl/fl}$;Mx1Cre mice treated with polyI:C. Lane 2, 5, 6, 7, and 8 were loaded with PCR products from polyI:C treated $Emcn^{fl/fl}$ mice, and exhibit bands of floxed *Emcn* (671 bp). The presence of this band and the absence of the KO band in lane 5-8 indicated that EMCN was not knocked out in polyI:C treated $Emcn^{fl/fl}$ mice. These lanes were representative for all polyI:C treated $Emcn^{fl/fl}$ mice, except for one. Lane 2 showed both the $Emcn^{fl}$ band (671 bp) and the KO band (302 bp), suggesting partly knock-out of EMCN. This result was highly unexpected; however, it persisted through several rounds of genotyping of this mouse.

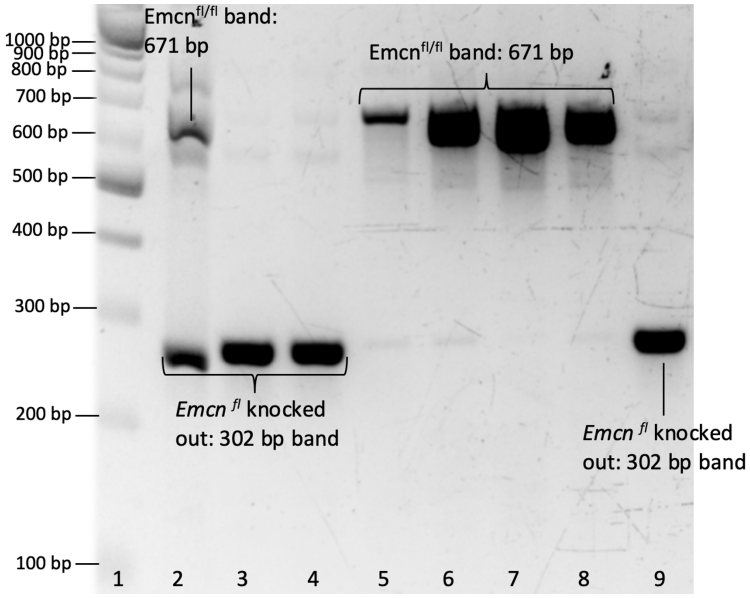

Figure 10: **Representative gel identifying knock-out of *Emcn* exon 1, 4 weeks post poly I:C treatment** The 100 base pair ladder (N3231) represents the first lane of the gel. The 302 bp band present in lane 2, 3, 4, and 9 contain DNA fragments of *Emcn* where exon 1 was knocked out. Lane 3, 4, and 9 were loaded with PCR products from poly I:C treated $Emcn^{fl/fl}$;Mx1Cre mice. DNA fragments of floxed *Emcn* constitute the 671 bp bands on the gel and are present in lane 2, 5, 6, 7, and 8. These lanes were loaded with PCR products from poly I:C treated $Emcn^{fl/fl}$ mice.

Now that it was confirmed that EMCN was indeed knocked out in polyI:C treated $Emcn^{fl/fl}$;Mx1Cre mice, the functional consequences of the knock-out could be assessed through transplantation assays. However, in order to investigate if the EMCN loss had any acute phenotype, FACS analysis was performed on EMCN KO and EMCN WT PB cells and BM cells prior to transplantation. To confirm that the hematopoietic system was at steady-state 4 weeks after the polyI:C treatment, blood count analysis was performed prior to the FACS analysis.

4.2 The effect of EMCN loss on steady state hematopoiesis

4.2.1 Blood count data confirm steady-state hematopoiesis 4 weeks after polyI:C treatment

PB from polyI:C treated $Emcn^{fl/fl}$;Mx1Cre and $Emcn^{fl/fl}$ mice, referred to as EMCN KO and EMCN WT mice, respectively, was analysed on a blood counter. The blood count data were then compared to previously acquired data from C57BL/6 mice in homeostasis. The comparison of blood count data from polyI:C treated mice with blood count data of untreated C57BL/6 mice was performed in order to confirm that the hematopoietic system had re-gained homeostasis after the polyI:C treatment. The blood count data from the EMCN KO and EMCN WT mice were also compared. This was done in order to assess whether EMCN loss had any effect on the frequency of the blood parameters that were analyzed. The level of WBC, RBC, HGB, hematocrit (HCT), and PLT for the different mice are shown in Figure 11. One-way ANOVA analysis with multiple comparisons revealed that there were no significant differences between the EMCN KO mice, the EMCN WT mice, or the C57BL/6 mice for any of the parameters ($p > 0.05$). The similar blood count values for the EMCN KO and the EMCN WT mice indicated that loss of EMCN did not affect the frequency of the blood parameters. Further, the similarity between these mice and the homeostatic C57BL/6 mice indicated that the hematopoietic system in the polyI:C treated mice was at steady-state 4 weeks after polyI:C treatment.

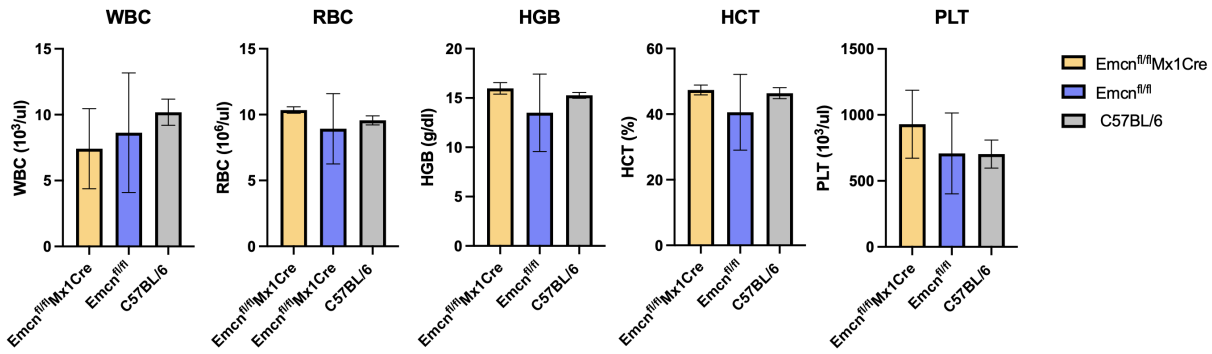

Figure 11: **Blood counts of EMCN KO mice, EMCN WT mice, and C57BL/6 mice.** The bar charts show the mean ± SD of the level of white blood cells (WBC) ($10^3/\mu$l), red blood cells (RBC) ($10^6/\mu$l), hemoglobin (HGB) (g/dl), hematocrit (HCT) (%), and platelets (PLT) ($10^3/\mu$l) in EMCN KO mice (n=5), EMCN WT mice (n=6), and C57BL/6 mice (n=3). The data were gender-matched.

Having confirmed that the hematopoietic system was at steady-state 4 weeks post polyI:C treatment, the functional consequences of EMCN loss in the HSCs was assessed.

4.2.2 FACS analysis of peripheral blood and bone marrow cells revealed no acute phenotype due to EMCN loss

To investigate if EMCN loss in the LT-HSCs exhibited any acute phenotype 4 weeks after the knock-out was induced, the frequency of PB cells, mature BM cells, and LT-HSCs in the mice were analyzed, before the transplantation assays were carried out. Antibody cocktails for surface markers allowed for the assessment of the mature blood cell types in the PB and BM, as well as for the LT-HSCs upon FACS analysis.

Isolation and analysis of PB cells

Upon the sacrifice of the EMCN KO and EMCN WT mice, PB was collected and analyzed on the LSR Fortessa (BD). Figure 12A shows representative FACS plots for the analysis of B cells, myeloid cells, and T cells from EMCN KO and EMCN WT peripheral blood collected from mice in exp. 2. The analysis is also representative of the mice in exp.1. B cells, myeloid cells (granulocytes and monocytes), and the T cells were assessed based on their surface expression of B220, Gr-1/CD11b, and CD3e, respectively. In the

representative plots, 64.5% and 57.5% B cells were detected in EMCN KO and EMCN WT mice, respectively. 21.0% (EMCN KO mouse) and 22.8% (EMCN WT mouse) cells were detected as myeloid cells, and 9.1% (EMCN KO mouse) and 11.2 % (EMCN WT mouse) cells were detected as T cells.

In order to determine whether EMCN loss in the LT-HSCs had affected the blood cell composition in the mice, the FACS data were quantified and compared. Figure 12B shows the average frequency of B220 positive cells (B cells), myeloid cells (Gr-1/CD11b positive), and CD3e positive cells (T cells) in PB from the mice. A t-test revealed no significant difference in the frequency of any of these populations in EMCN KO mice vs. EMCN WT mice. This suggested that EMCN does not affect the LT-HSC's capacity for multi-lineage blood production. However, since the EMCN KO only had been present for 4 weeks at the time of the analysis, and because many mature blood cells have a life span exceeding that of this period, conclusions could not be drawn from this analysis alone.

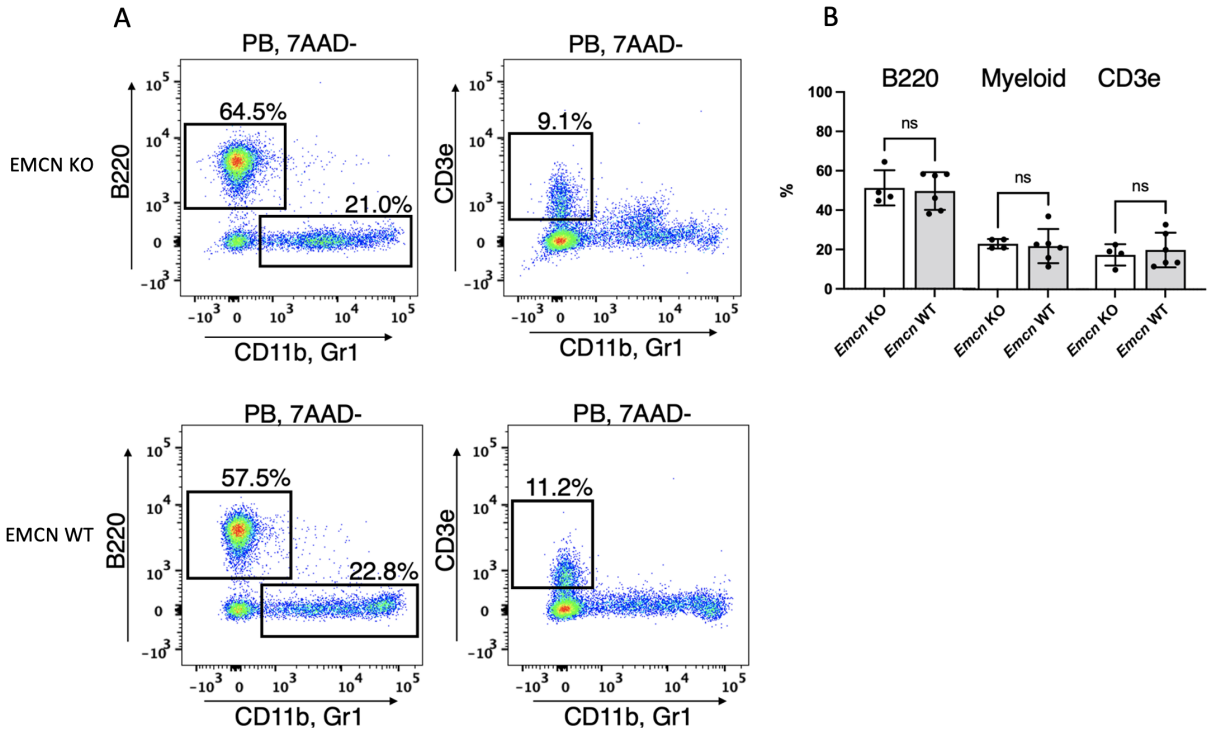

Figure 12: **FACS analysis of mature peripheral blood cells 4 weeks post polyI:C treatment (A)** Representative FACS plots showing the distribution of B cells, myeloid cells, and T cells in PB of EMCN KO and EMCN WT mice (exp. 2), 4 weeks post polyI:C treatment. B cells, myeloid cells, and T cells were isolated from live (7AAD$^-$) PB cells based on their positive surface expression of B220, CD11b/Gr-1, and CD3e, respectively. **(B)** Quantification of the PB FACS data for all polyI:C treated mice in exp. 2. The bar chart shows the mean ± SD percentage of B220$^+$ cells (B-cells), myeloid cells (Gr-1/CD11b$^+$), and T cells (CD3e$^+$) in the PB of the EMCN KO and the EMCN WT mice. T-test demonstrates no significant ($p > 0.05$) differences between the frequency of any of the blood cells comparing the EMCN KO (n=4) mice with the EMCN WT (n=6) mice.

Isolation and analysis of mature BM cells

WBM cells collected from EMCN KO and EMCN WT mice were analyzed on the LSR Fortessa (BD), following antibody staining. As for the PB analysis, mature B cells, myeloid cells, and T cells were isolated from live cells (7AAD$^-$) based on their surface expression of B220, Gr-1/CD11b, and CD3e, respectively.

Representative FACS plots for the analysis of the mature BM cells from EMCN KO

and EMCN WT mice in exp. 1 are shown in Figure 13A. The analysis is also representative for the mice in exp. 2. In the representative FACS plots, 21% (EMCN KO) and 14% (EMCN WT) of the BM cells were assessed as B cells based on positive surface expression of B220. 49% (EMCN KO) and 48% (EMCN WT) myeloid cells were assessed based on surface marker expression of CD11b/Gr-1, and 1.5% (EMCN KO) and 1.3% (EMCN WT) cells were assessed as T cells based on positive expression of CD3e.

To investigate if the loss of EMCN had affected the BM composition in terms of cell frequency or lineage skewing after 4 weeks, the FACS data were quantified and compared. Figure 13B shows the average percentage of B cells, myeloid cells, and T cells in WBM from EMCN KO and EMCN WT mice. A t-test revealed no significant difference between the frequency of the cells comparing the EMCN KO mice with the EMCN WT mice. As for the result of the PB analysis, this indicated that EMCN expression in LT-HSCs does not affect blood cell production. However, to conclude on the consequence of EMCN loss, the samples had to be examined for a more extended period transplantation assays.

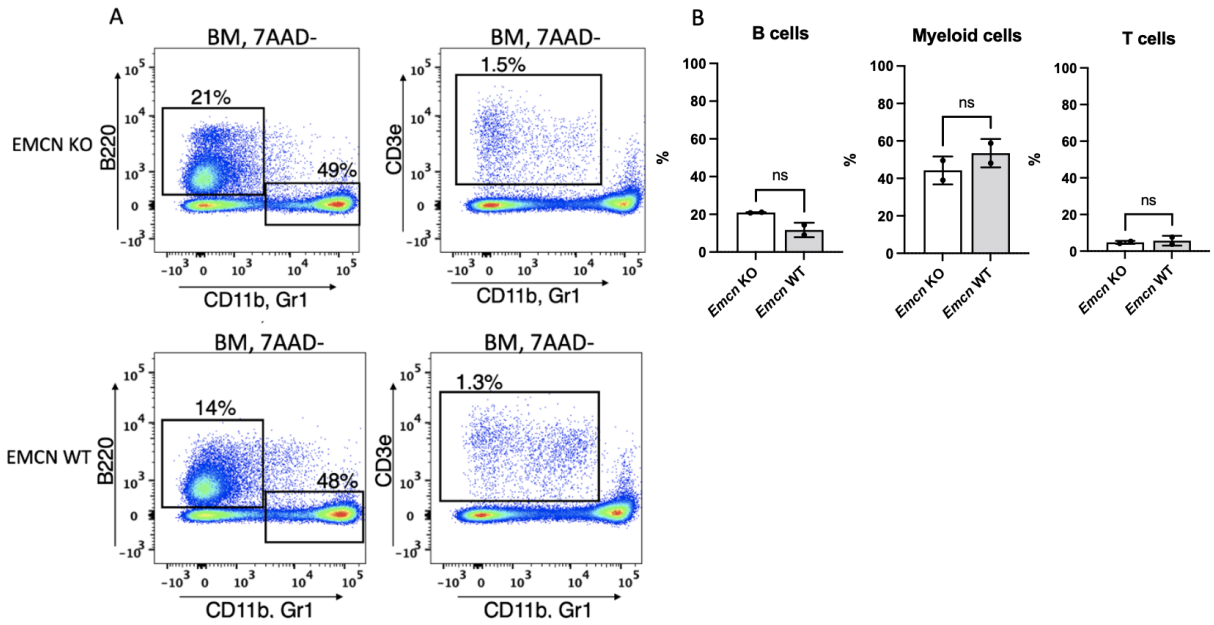

Figure 13: **FACS analysis of mature bone marrow cells 4 weeks post polyI:C treatment (A)** Representative FACS plots for the analysis of B cells, myeloid cells, and T cells in the BM of EMCN KO and EMCN WT mice 4 weeks after polyI:C treatment. The B cells, myeloid cells, and the T cells were isolated from live BM cells ($7AAD^-$) based on positive surface expression of B220, CD11b/Gr-1, and CD3e, respectively. **(B)** Quantification of the FACS analysis of mature BM cells from EMCN KO and EMCN WT mice. The mean ± SD percentage of B cells, myeloid cells, and T cells in WBM from EMCN KO (n=2) and EMCN WT (N=2) mice are presented in the bar chart. T-test revealed no significant ($p > 0.05$) difference between the frequency of either cell type in the EMCN KO compared to the EMCN WT mice.

FACS analysis and sorting of LT-HSCs for transplantation

The functional role of EMCN in adult HSCs has not yet been characterized. To investigate the function of EMCN within the LT-HSC compartment, EMCN KO and EMCN WT LT-HSCs were sorted and functionally analyzed in a transplantation assays. Following lineage depletion of $5x10^6$ WBC, LT-HSCs were sorted on the BD FACS Aria III (BD) based on their protein surface expression identified by antibody staining.

Figure 14A shows representative FACS plots demonstrating the frequency of LT-HSCs in the mice, as well as the gating strategy used to isolate these cells. To gate out the LT-

HSCs, live ($7AAD^-$) $lineage^-$ Kit^+ cells were selected from single BM cells. These cells constituted 7.5 % (EMCN KO) and 8.1% (EMCN WT) of the cells in the representative plots. Subsequently, the Kit^+ and $Sca\text{-}1^+$ cells (LSKs), were assessed (0.99% (EMCN KO) and 2.2% (EMCN WT) in the representative plots), before the cell population containing the LT-HSC frequencies of the LSKs were analyzed based on the presence of CD150 and absence of CD48. 15.2% (EMCN KO) and 11.2% (EMCN WT) of the LSKs in the presented plots were isolated as LT-HSCs.

To investigate if the EMCN loss had influenced the frequency of LT-HSCs in the mice, the FACS data were quantified. The average percentage of LT-HSCs in the ($7AAD^-$) $lineage^-$ population in the EMCN KO and EMCN WT mice is presented in Figure 14B. A t-test demonstrated that there was no significant difference between the frequency of LT-HSCs in the EMCN KO mice compared to the EMCN WT mice. This suggested that EMCN is not essential for LT-HSC maintenance. Prior to transplanting the LT-HSCs into recipient mice, the FACS sorting was re-analyzed to confirm that the sorted cells were indeed LT-HSCs. A representative FACS plot for the re-analysis of sorted cells is presented in figure 14C, demonstrating that the sort was successful. The re-analysis shows that the majority of the sorted cells were in the LT-HSCs population (LSK $CD150^+CD48^-$).

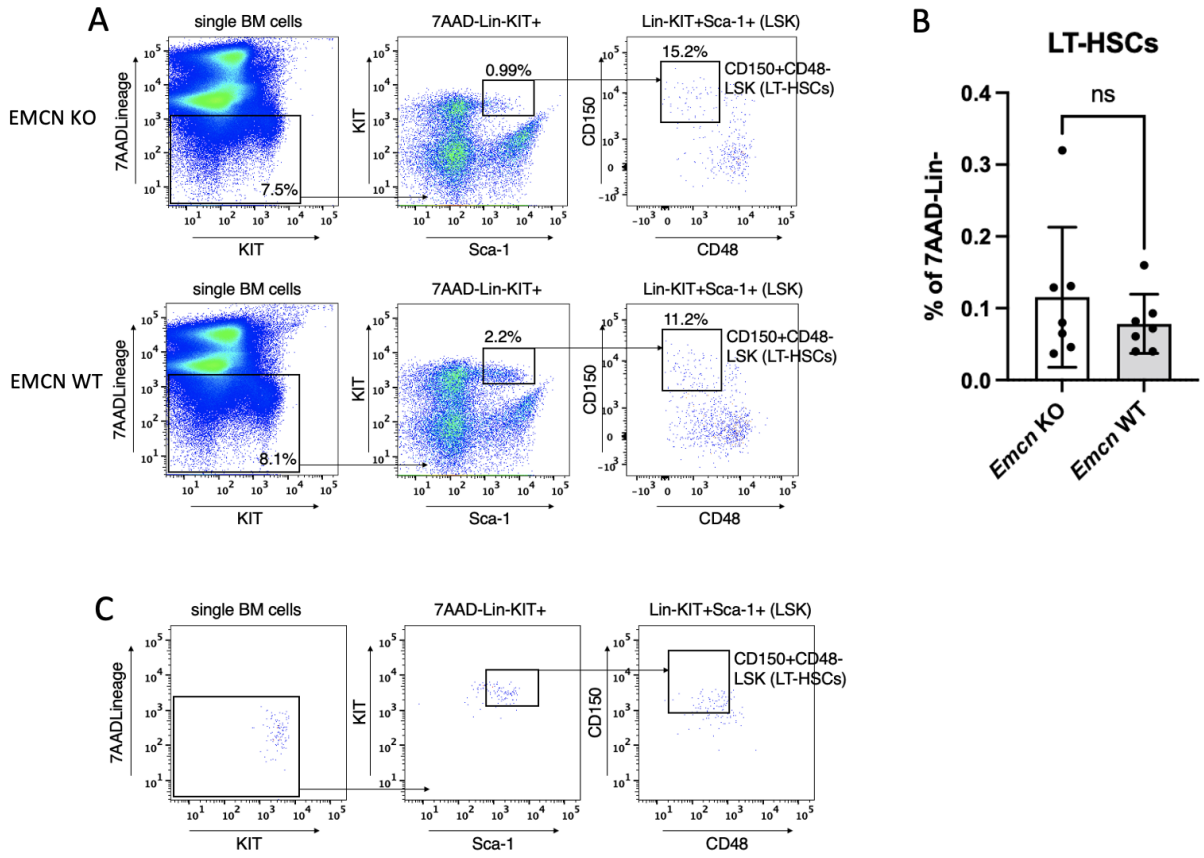

Figure 14: **FACS analysis and sort of LT-HSCs from EMCN KO and EMCN WT mice (A)** Representative FACS plots showing the distribution of LT-HSCs in EMCN KO and EMCN WT mice. To isolate the LT-HSC population, live(7AAD$^-$) lineage$^-$ Kit$^+$ cells were selected from single lineage depleted BM cells. **(B)** Quantification of the LT-HSC frequencies in EMCN KO and EMCN WT mice. The bar chart presents the mean ± SD percentage of LT-HSCs in the 7AAD$^-$ Lin$^-$ population of the mice. A t-test revealed no significant difference ($p > 0.05$) of LT-HSCs frequencies between the EMCN KO (n=7) mice and the EMCN WT (n=7) mice. **(C)** Representative FACS plot showing re-analysis of sorted LT-HSCs. The re-analysis demonstrates that the majority of the sorted cells were CD150$^+$ CD48$^-$LSKs.

Following the phenotypic analysis of the LT-HSC compartment suggesting that EMCN is not essential for sustaining LT-HSC frequencies, its role in maintaining quiescence of LT-HSCs was investigated. To study the effect of EMCN loss on LT-HSC cell cycle state, cell cycle analysis was performed using the LSR Fortessa (BD).

4.2.3 Cell cycle analysis suggests that EMCN does not affect HSC quiescence

During homeostasis, the LT-HSCs are in a quiescent state facilitating the life-long maintenance of the HSC population size as well as the production of all mature blood cell lineages [37]. To further investigate the function of EMCN for LT-HSCs, the role of EMCN in maintaining LT-HSC quiescence was investigated by cell cycle analysis. Following antibody staining, $5x10^6$ lineage depleted cells were fixed and permeabilized before they were stained with DAPI and Ki-67 antibody conjugated to FITC. Analysis based on the presence of the nuclear proliferation-associated protein, Ki-67, and the quantity of cellular DNA, allowed for the distinction between cells in G_0, G_1, and S-G_2M phase of cell cycle.

Figure 15A shows representative FACS plots for the isolation of EMCN KO and EMCN WT LT-HSCs in G_0, G_1, and S-G_2M phase. LSKs were first isolated from live ($7AAD^-$) $lineage^-$ Kit^+ cells (0.69% (EMCN KO) and 0.57% (EMCN WT) cells in the representative plots) before the cell population containing the LT-HSCs was gated out from the LSKs based on $CD150^+CD48^-$surface marker expression. 6.56% (EMCN KO) and 15.4% (EMCN WT) LT-HSCs were selected in the representative plots. The cell cycle state was then assessed in the LT-HSCs.

Cells in G_0 phase have only one set of diploid chromosomes, and they do not express the Ki-67 antigen. These cells could therefore be gated out based on low DAPI signal intensity and the absence of Ki-67 signal. 68.9% of the EMCN KO LT-HSCs and 83.8% of the EMCN WT LT-HSCs in the representative plot were in G_0 phase. Cells in G_1 phase are also $DAPI^{Low}$; however, they express Ki-67, which was used to distinguish them from the G_0 population before they were assessed (19.8% (EMCN KO) and 12.3% (EMCN WT) in the representativ plots). Cells in S-G_2M phase synthesize DNA and thus have higher DNA content compared to cells in G_0 and G_1 phase. A high DAPI signal combined with the presence of Ki-67 was utilized to isolate these cells (7.55% (EMCN KO) and 2.6% (EMCN WT) in the representative plots) [99].

To assess whether EMCN affects quiescence in LT-HSCs, the FACS data were quantified. Figure 15B show the average percentage of EMCN KO and EMCN WT LT-HSCs

in G_0, G_1, and S-G_2M phase. The bar chart demonstrates that only about 70% of the LT-HSCs were in G_0 phase 4 weeks post polyI:C treatment, which was surprisingly low comparing it to the literature stating that about 90-95% of HSCs are quiescent during steady-state hematopoiesis [37]. A t-test was performed to assess whether there was any difference in the frequency of cells in the different stages comparing the EMCN KO and the EMCN WT LT-HSCs. However, the test demonstrated that there was no significant difference between the two groups. This suggested that EMCN is not crucial for maintaining quiescence in LT-HSCs.

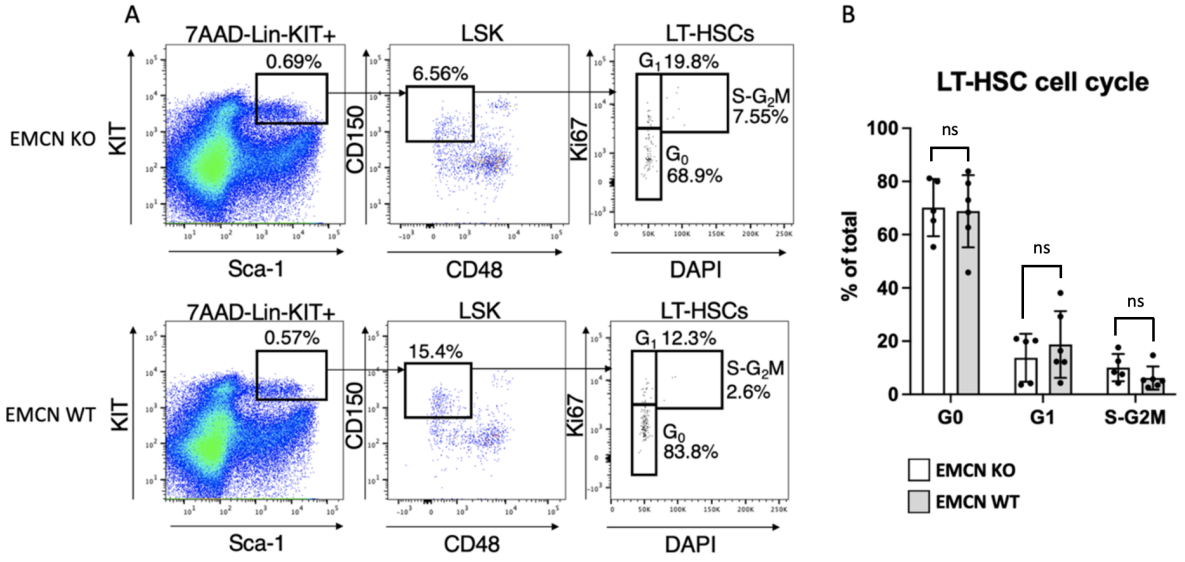

Figure 15: **Cell cycle analysis of EMCN KO and EMCN WT LT-HSCs (A)** Representative FACS plots showing the distribution of EMCN KO and EMCN WT LT-HSCs in G_0, G_1, and S-G_2M phase of the cell cycle. To isolate the LT-HSCs, Kit$^+$ Sca-1$^+$ cells (LSKs) were selected from live (7AAD$^-$) lineage$^-$ Kit$^+$ EMCN KO and EMCN WT BM cells, before CD150$^+$CD48$^-$ LT-HSCs were assessed. From the LT-HSCs cells in G_0 phase were assessed based on DAPI ^{low} and Ki-67^{low}, cells in G_1 were assessed as DAPI^{low} and Ki-67^{high}, and cells in S-G_2M phase were assessed as DAPI^{high} and Ki-67^{high}. **(B)** Quantification of the cell cycle FACS data. The bar chart presents the mean ± SD percentage of EMCN KO (n=5) and EMCN WT (n=6) LT-HSCs in G_0, G_1, and S-G_2M phase of the cell cycle. T tests revealed that there was no significant difference ($p > 0.05$) between the EMCN KO and the EMCN WT.

Despite the analysis of the frequency of PB cells and BM cells, as well as the analysis

of the cell cycle state of the LT-HSCs, no phenotype related to the loss of EMCN was observed. However, as discussed earlier, the consequence of EMCN loss needs to be studied for a more extended period to draw any conclusions regarding the phenotype of EMCN loss in HSCs. Also, to exclude the possible contribution from other EMCN KO BM cells, the cell-autonomous function of EMCN had to be studied in WT microenvironment. To further study the function of EMCN in LT-HSCs, LT-HSC transplantation assays were carried out.

4.3 Long-term HSC transplantation assay

To date, HSC transplantation assays are the only functional assays that can prove whether a cell is a true long-term repopulating stem cell [1]. To study whether EMCN expression in LT-HSCs affects their capacity to reconstitute the hematopoietic system of lethally irradiated mice, LT-HSC transplantation was performed.

200 EMCN KO or EMCN WT LT-HSCs (CD45.2) were sorted and transplanted into triplicates of lethally irradiated wild-type recipients (CD45.1) together with 200,000 WBM support cells (CD45.1). 200,000 WBM cells contain a maximum of 10 LT-HSCs [32], meaning that the ratio of CD45.2 and CD45.1 LT-HSCs transplanted was about 20:1. During the project, the LT-HSC transplantation assay was carried out twice. In the first transplantation assay (exp. 1), LT-HSCs from 2 EMCN KO mice and 1 EMCN WT mouse were transplanted. The intention was to transplant cells from 2 EMCN WT mice, however, genotyping demonstrated that one of the two polyI:C treated $Emcn^{fl/fl}$ mice were positive both for the $Emcn^{fl/fl}$ sequence and the *Emcn* exon 1 KO sequence (Figure 10, lane 2). Because of the unclear genotype, this mouse was not used for transplantation. In the second transplantation assay (exp. 2), 5 EMCN KO mice and 6 EMCN WT mice were used for transplantation. During the assays, most of the mice got skin lesions on their neck due to X-ray irradiation. X-ray irradiation was used because the Gammacell irradiator was not available due to required service by the time of transplantation assays. After regular nail cutting to prevent itching and treatment with Isaderm Vet. cream, most mice survived. However, in exp. 1, one mouse that was transplanted with EMCN KO cells, and two mice transplanted with EMCN WT cells had to be sacrificed due to

suffering caused by the skin lesions. In exp. 2, two mice transplanted with EMCN KO cells and 8 mice transplanted with EMCN WT cells were sacrificed due to suffering caused by the skin lesions.

4.3.1 FACS analysis of PB cells suggests that blood production in the recipients is not dependent on EMCN activity in donor LT-HSCs

To assess whether EMCN KO LT-HSCs have the capacity to reconstitute the hematopoietic system, the frequency of donor derived PB cells of the recipients was analyzed by FACS every fourth week. In exp. 1, blood samples were collected 4, 8, 12, and 16 weeks post transplantation. Exp. 2 was still running by the end of this thesis; however, blood was analyzed at 8, and 12 weeks. PB was not collected and analyzed at 4 weeks due to lesions in the neck of the mice. Prior to the FACS analysis, the PB cells were subjected to antibody staining for PB cells.

Figure 16A shows FACS plots representative for recipients transplanted with EMCN KO or EMCN WT LT-HSCs in exp.2 and demonstrates donor-derived engraftment in the mice 12 weeks after transplantation. FACS plot 1 demonstrates how donor-derived PB cells were gated based on their expression of CD45.2. In this plot, 72% of the PB cells were donor-derived. This number is not representative for the frequency of donor-derived cells in recipients from exp. 1, which is not presented due to low engraftment of less than 5%. The low engraftment was related to technical issues of the transplantation procedure, and it needs to be repeated.

In order to compare engraftment in the recipients transplanted with EMCN KO and EMCN WT LT-HSCs, the FACS data generated at each time point were quantified. The bar charts in Figure 16B show the average percentage of donor derived PB cells in exp. 2, at 12 weeks post transplantation. Both groups of recipients exhibited about 60% donor-derived PB cells, which indicated that the transplantation was successful considering similar frequencies observed preciously in the lab following transplantation of donor LT-HSCs (CD45.2) and LT-HSCs from support cells (CD45.1) in 20:1 ratio, respectively. Further, the high frequency of donor-derived PB cells in the recipients from exp. 2

suggested that both the EMCN KO and the EMCN WT LT-HSCs had the capacity to repopulate the hematopoieitc system of the recipients. The plot for exp. 1 at 12 weeks is shown in Supplementary Figure 1A (Appendix 2), and demonstrates only 5% donor-derived PB cells. T-tests comparing donor derived engraftment in recipients transplanted with EMCN KO, and EMCN WT LT-HSCs were performed for each time point during the assays. These demonstrated that there was no significant difference ($p > 0.05$) in the frequency of donor derived PB cells comparing the two groups of recipients. Hence, the result suggested that the LT-HSC's ability to reconstitute the hematopoietic system is not dependent on EMCN.

In order to assess engraftment capacity over time, the quantified FACS data from each time point were put in one graph. The average percentage of donor derived PB cells in the recipients from exp. 2 are shown as a function of time in Figure 16C. As anticipated, the frequency of donor derived PB cells in exp. 2 increased during the transplantation assay as the donor LT-HSCs started to proliferate. This was not observed in the recipients from exp. 1 (Supplementary Figure 1B, Appendix 2), which was unexpected. As for the poor engraftment observed in this transplantation assay, this was most probably due to technical issues related to the transplantation procedure.

To study whether the lack of EMCN had any effect on engraftment in terms of lineage skewing, donor derived B cells ($B220^+$), myeloid cells ($CD11b^+Gr\text{-}1^+$), and T cells ($CD3e^+$) were assessed by FACS analysis. FACS plots representative for the frequency of these cell types in recipients from exp. 2 (12 weeks) are shown in Figure 16A (FACS plot 2 and 3). In the representative FACS plot, 36% of the donor derived PB cells were B cells, 45% were myeloid cells, and 18% were T cells. The FACS data were quantified, and t-tests were performed to compare the average frequencies of B cells, myeloid cells, and T cells derived from EMCN KO and EMCN WT LT-HSCs. The quantified data are presented in Figure 16D. A t-tests revealed that there was no significant difference between the frequency of any of the cell types comparing the two groups of recipients. This indicated that EMCN does not affect engraftment in terms of lineage skewing.

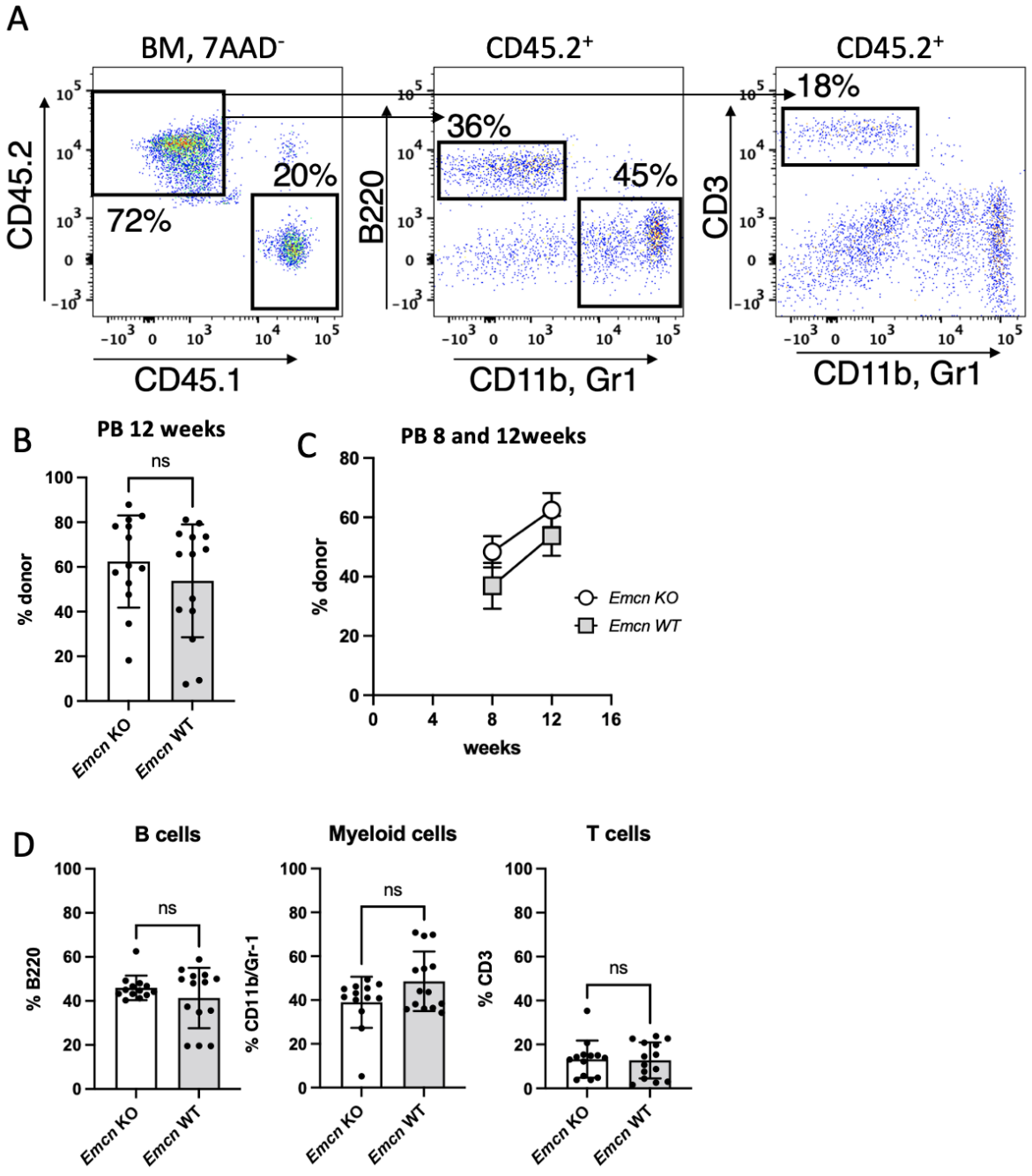

Figure 16: **FACS analysis of PB cells during LT-HSC transplantation assays (exp.2). (A)** FACS plots representative for the distribution of donor derived B cells ($B220^+$), myeloid cells ($CD11b^+/Gr\text{-}1^+$), and T cells ($CD3e^+$) in the PB of recipients transplanted with EMCN KO or EMCN WT LT-HSCs in exp. 2, 12 weeks post transplantation. **(B)** Quantification of FACS analysis for donor derived PB cells in recipient mice from exp. 2- 12 weeks after transplantation. The graph shows the mean ± SEM of the percentage of donor derived PB cells in recipient mice transplanted with EMCN KO (n=13) and EMCN WT LT-HSCs (n=10). (Figure text continues on the next page).

About 60% of the PB cells in the recipient mice were donor derived. T-test shows no significant difference ($p > 0.05$) in the percentage of donor derived PB cells between the two groups of recipients. **(C)** Quantified FACS data for donor derived PB cells (CD45.2) in recipient mice from epx. 2- 8 and 12 weeks after transplantation. The graph shows the mean ± SEM of the percentage of donor derived PB cells as a function of time. **(D)** Quantified FACS data for donor derived B cells, myeloid cells, and T cells in recipients from exp. 2- 12 weeks into the assay. The graph demonstrates the mean ± SEM of the percentage of donor derived cells. T-test demonstrates no statistical difference ($p > 0.05$) in any of the cell types between recipients transplanted with EMCN KO and EMCN WT LT-HSCs.

4.3.2 FACS analysis of recipient BM cells indicates that EMCN expression by LT-HSCs is not essential for their capacity to repopulate the BM

16 weeks after transplantation, upon the termination of the assay (exp.1), BM cells were collected and analyzed on FACS following preparation and antibody staining for WBM cells and LT-HSCs. In addition to the typical staining for WBM cells and LT-HSCs, the cells were stained with CD45.2 allowing the study of donor derived cells. This was done to investigate the effect of EMCN loss on BM engraftment.

As for the PB cell analysis, donor derived mature BM cells were assessed based on CD45.2 expression (FACSs plot not shown). Figure 17 shows the quantification of the FACS data. A t-test performed to compare the frequency of donor derived BM cells in the two groups of recipients demonstrated that there was no significant difference. This suggested that EMCN activity in LT-HSCs is not essential for the LT-HSCs to repopulate the bone marrow of lethally irradiated recipients. However, similar to what was observed in the PB analysis, the number of donor derived cells was unexpectedly low, constituting only about 2% of the recipient BM. This highly deviates from the 80-100% donor-derived BM cells, which normally is observed in the lab at the 16 week's time point in such transplantation assay. Due to low engraftment, exp. 2 was initiated shortly after the low engraftment in exp. 1 was observed.

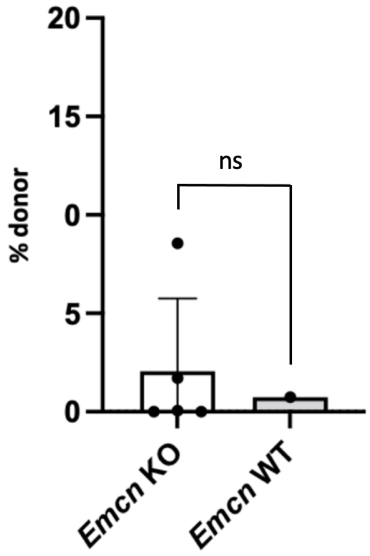

Figure 17: **FACS analysis of mature BM cells upon termination of the LT-HSC transplantation assay (exp. 1)** Quantified FACS data for the analysis of donor derived mature BM cells 16 weeks after transplantation. The bar chart shows the mean ± SEM percentage of donor derived BM cells in recipients transplanted with EMCN KO (n=4) and EMCN WT (n=1) LT-HSCs. 1-2.5% of the BM cells are donor derived. T-test revealed that there was no statistical difference ($p > 0.05$) between the EMCN KO and the EMCN WT.

The FACS analysis of the donor LT-HSCs revealed no EMCN protein expression, neither in the EMCN KO LT-HSCs nor in the EMCN WT LT-HSCs (CD45.2) in the recipients. This was highly unexpected, and the possible lack of protein expression was further investigated.

Taken together, ignoring the possibility that the intended control did not express EMCN, the data obtained during the transplantation assay suggested that EMCN activity in LT-HSCs is not essential for their capacity to reconstitute the hematopoietic system. However, to further confirm the result, a competitive transplantation assay was initiated.

4.4 Competitive transplantation assay

A competitive transplantation assay was established to compare engraftment capacity of EMCN KO and EMCN WT LT-HSC. In competitive transplantation assays, the function of HSCs possessing different genotypes can be compared directly to that of competitor HSCs. This improves the sensitivity of the transplantation assay and allows for an internal technical control minimizing the effect of potential disparate irradiation and injection [100]. For the sake of preventing any possible effects of the EMCN KO on the LT-HSC's ability to home in the BM, the intention was to treat the recipients with polyI:C following transplantation into WT recipient mice (CD45.1). From 6 targeted donor mice, 250,000 WBM cells were transplanted along with 250,000 WT WBM cells (CD45.1) into triplicates of lethally irradiated recipients. Unfortunately, the mice had to be sacrificed due to severe lesions in the neck, resulting from the X-ray irradiation, before the KO was induced.

4.5 Confirmation of the knock-out

Summarizing the findings, no phenotype of EMCN could be revealed, neither through the analysis of PB cells and BM cells 4 weeks after inducing the KO, nor in the transplantation assays. However, when analysing donor-derived LT-HSCs in the transplanted recipients, no EMCN expression could be seen. Similar findings were also observed earlier in the project when analyzing EMCN expression in LT-HSCs from polyI:C treated mice (analysis shown in the next paragraph). However, the result of this assay suggesting lack of EMCN expression in the polyI:C treated $Emcn^{fl/fl}$ mice was not considered reliable at this point and the transplantation assays were carried out. The reason the result was not believed was because genotyping performed after the induction of the KO had revealed that *Emcn* exon 1 was only knocked out in the $Emcn^{fl/fl}$;Mx1Cre mice, and not in the controls. In addition, different EMCN antibodies possessing varying binding efficiency were tested in the lab prior to the project, and it was assumed that the wrong EMCN antibody could have been used for the staining. However, prior to the analysis of the donor-derived LT-HSCs form the recipients in the transplantation assay, sufficient binding efficiency of the chosen antibody were confirmed by testing it on LT-HSCs from

C57BL/6 mice, to exclude any doubt regarding the reliability of the staining.

4.5.1 LT-HSCs in polyI:C treated *Emcn*$^{fl/fl}$ mice do not express EMCN

LT-HSCs from polyI:C treated mice and recipients transplanted with EMCN KO and EMCN WT LT-HSCs were analyzed by FACS upon antibody staining for EMCN. Figure 18 shows representative FACS plots for the analysis of LT-HSCs in lineage depleted BM cells 4 weeks after polyI:C treatment. The FACS plots are also representative for the analysis of EMCN expressing LT-HSCs carried out upon the termination of the transplantation assay (exp.1). The LT-HSCs were assessed as LSK CD150^{+}CD48^{-} cells and subjected to analysis of EMCN expression. The FACS plots demonstrated that there was no EMCN expression in the EMCN KO LT-HSCs (i.e., *Emcn*$^{fl/fl}$;Mx1Cre), which was as anticipated, nor in the EMCN WT LT-HSCs (i.e., *Emcn*$^{fl/fl}$), which was highly unexpected.

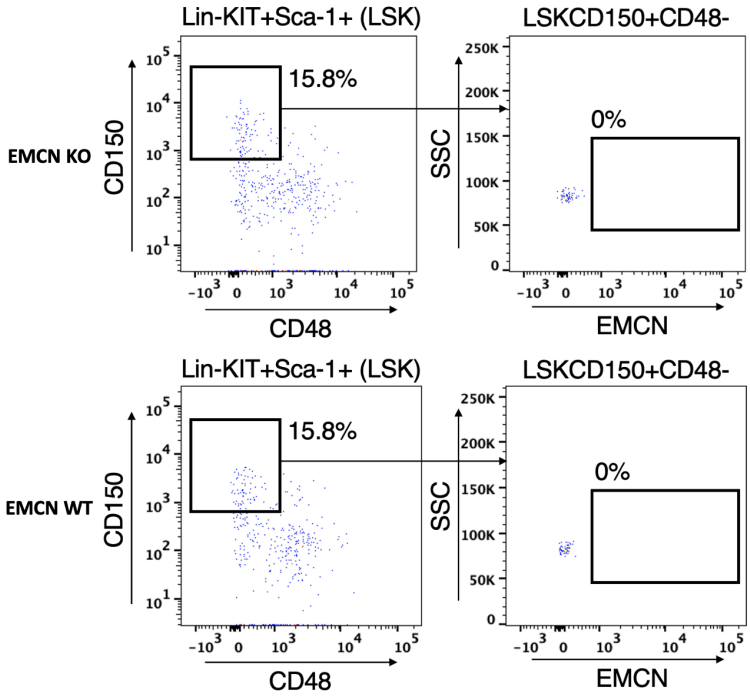

Figure 18: **Analysis of EMCN expression in LT-HSCs from polyI:C treated mice**. Representative FACS plots for the analysis of EMCN$^+$ LT-HSCs in *Emcn*$^{fl/fl}$;Mx1Cre and *Emcn*$^{fl/fl}$ mice 4 weeks after polyI:C treatment. In the representative plots, 15.8% LT-HSCs were isolated from the LSK population of cells from EMCN KO and EMCN WT mice based on CD150$^+$CD48$^-$ surface expression. EMCN expression was further analyzed in the LT-HSCs based on EMCN signal and SSC. Neither EMCN KO LT-HSCs nor EMCN WT LT-HSCs expresses EMCN.

Two separate analyses of EMCN expression in LT-HSCs have now confirmed that EMCN was knocked out on protein level in the polyI:C treated *Emcn*$^{fl/fl}$ mice. This finding was highly contradictory to the genotyping result obtained post polyI:C treatment demonstrating that the *Emcn* was not knocked out on the gene level in these mice. In order to understand what caused the lack of EMCN protein expression in the control mice, further investigation was carried out.

4.5.2 PolyI:C treatment do not effect EMCN expression mice

To investigate if the lack of EMCN expression in the EMCN WT mice could be explained by unknown effects of the polyI:C treatment, the effect of the drug was studied in C57BL/6 mice. 3 C57BL/6 mice were treated with polyI:C employing the treatment

strategy used for the targeted mice. Additionally, 3 C57BL/6 mice were treated with PBS serving as controls. 4 weeks after the treatment, BM was collected from the mice, and FACS analysis was performed following antibody staining for LT-HSCs and EMCN. Figure 19A shows representative FACS plots for the analysis of EMCN expressing LT-HSCs (LSK $CD150^{+}CD48^{-}EMCN^{+}$) from the polyI:C treated and PBS treated C57BL/6 mice, from which 65% and 61% were EMCN positive, respectively. The quantification of the FACS data, shown in Figure 19B. A t-test revealed that the average percentage of LSKs (*), LT-HSCs (**), and $EMCN^{+}$LT-HCSs (*) in the lineage negative population was significantly lower in the polyI:C treated mice. This was as expected, knowing that polyI:C induces an inflammatory state in the mice [97], which is associated with LT-HSC cell cycle entry [37]. However, the quantified FACS data and a t-test revealed that the percentage of LT-HSCs expressing EMCN in the mice was not reduced by the polyI:C treatment. This demonstrated that the lack of EMCN expression in the EMCN WT mice could not be explained by the polyI:C treatment.

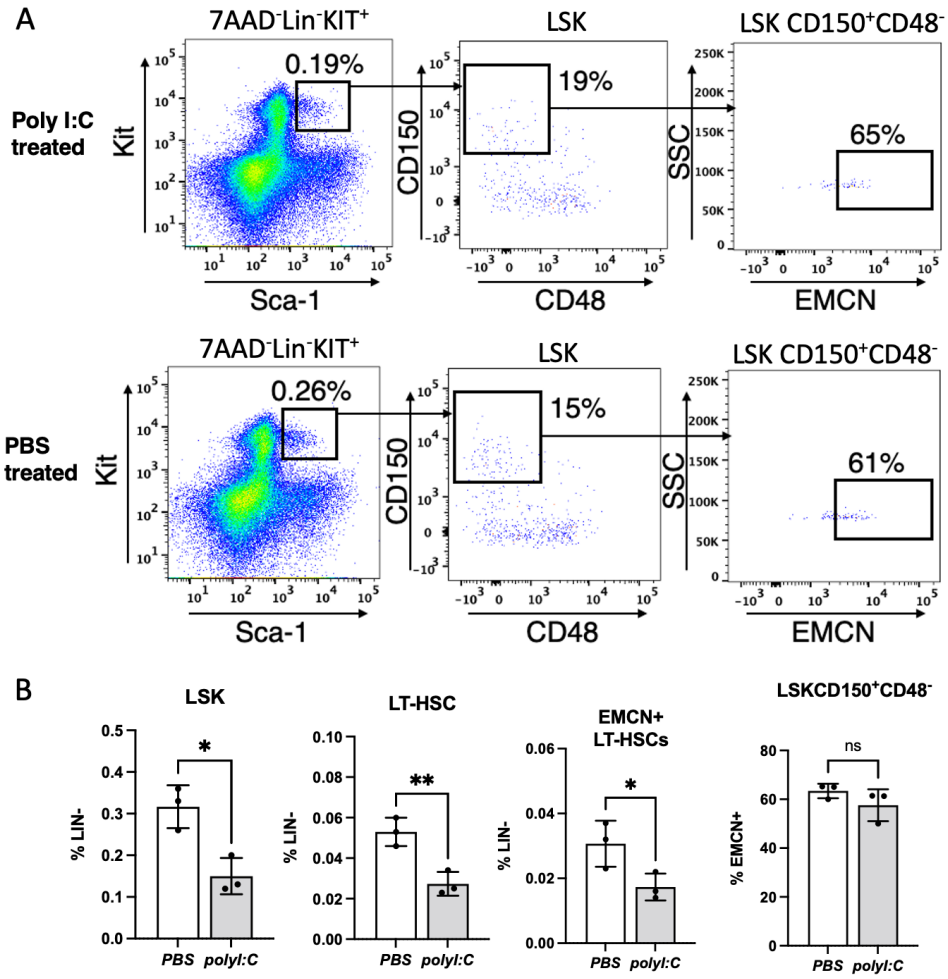

Figure 19: **FACS analysis of EMCN expressing LT-HSCs in polyI:C and PBS treated C57BL/6 mice. (A)** Representative FACS plots demonstrating the frequency of EMCN$^+$ LT-HSCs in the mice. To isolate the LT-HSCs, the LSKs (Lin$^-$Sca-1$^+$Kit$^+$) were first gated out from the 7AAD$^-$Lin$^-$Kit$^+$ population of cells (0.19% for polyI:C treated and 0.26% for PBS treated mice, respectively). The LT-HSCs were assessed as CD150$^+$CD48$^-$ LSKs (0.19% and 0.15% for the polyI:C and PBS treated mice, respectively). In the representative plots, 65% and 61% of the LT-HSCs from polyI:C and PBS treated mice, respectively, were EMCN positive. **(B)** Quantification of the FACS data demonstrating the mean ± SD percentage of LSKs, LT-HSCs, and EMCN$^+$LT-HSCs in the lin$^-$ population, and the percentage of LT-HSCs in the EMCN$^+$ population of polyI:C treated (n=3) and PBS treated (n=3) mice. T-test revealed that the frequency of LSKs (*), LT-HSCs (**), and EMCN$^+$LT-HSCs (*) was significantly lower in polyI:C treated C57BL/6 mice compared to PBS treated mice. T-test revealed no statistical difference ($P > 0.05$) in the percentage of EMCN$^+$LT-HSCs in polyI:C treated C57BL/6 mice as compared to PBS treated mice. (*) $P < 0.05$; (**) $P < 0.01$.

Since the lack of EMCN expression in the control mice could not be explained by the polyI:C treatment, it was suspected that the LoxP sequences targeted to exon 1 might have interfered with the protein expression. To investigate this theory, EMCN expression in LT-HSCs from targeted mice that were not treated with polyI:C was investigated.

4.5.3 EMCN is not expressed in exon 1 targeted mice regardless of polyI:C treatment

BM was collected from 4 $Emcn^{fl/fl}$;Mx1Cre mice, 4 $Emcn^{fl/fl}$, and 1 C57BL/6 mouse, not treated with poly I:C. Following antibody staining for LT-HSCs and EMCN, FACS analysis was performed. Figure 20 shows representative FACS plots for the analysis of EMCN expression in the LT-HSCs from the mice. GMPs (LK CD150$^-$ CD16/32$^+$), which do not express EMCN, were used as a control population to set the positive gate for EMCN expression [81]. The GMP population in the mice used to set the gating is shown in the lower part of the figure. The analysis demonstrated that 84% of the LT-HSCs from the C57BL/6 mouse expressed EMCN, which was used to set the baseline for EMCN expression. Since the knock-out had not been induced in the mice, the $Emcn^{fl/fl}$;Mx1Cre mice and $Emcn^{fl/fl}$ mice were expected to exhibit the same level of EMCN expression as the C57BL/6 mouse. However, the analysis revealed that the LT-HSCs from these mice exhibited no EMCN expression. This indicated that the LoxP sites targeting exon 1 of *Emcn* had interfered with the expression of the protein.

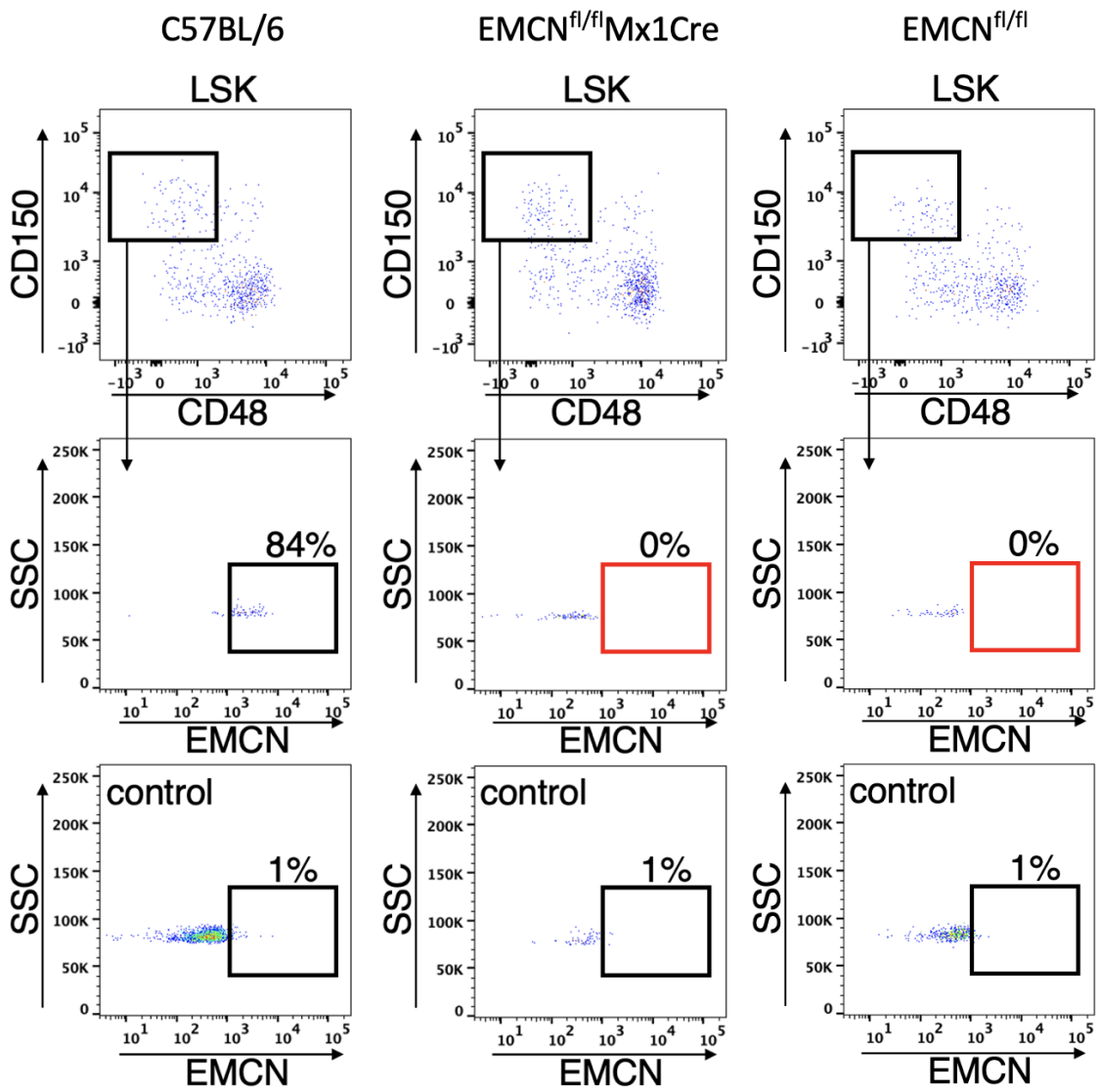

Figure 20: **FACS analysis of EMCN expression in LT-HSCs from C57BL/6 mouse, *Emcn*$^{fl/fl}$;Mx1Cre mice, and *Emcn*$^{fl/fl}$ mice.** Representative FACS plots showing the level of EMCN expression in C57BL/6 mouse and targeted mice, not treated with polyI:C. In the lower part of the figure, control populations of GMPs are shown. GMPs do not express EMCN and were used to set the positive gates for EMCN expression. The LT-HSCs in the mice were assessed as CD150^{+}CD48^{-} LSKs. 84% of the C57BL/6 LT-HSCs expressed EMCN, whereas 0 % of the LT-HSCs from the *Emcn*$^{fl/fl}$;Mx1Cre and *Emcn*$^{fl/fl}$ mice exhibited positive EMCN expression.

After confirming that the EMCN protein expression was knocked out in targeted mice regardless of whether the KO was induced or not, RT-qPCR was performed to investigate whether *Emcn* was expressed at the mRNA level. This was carried out to determine if the

targeting of exon 1 could have interfered with the transcription of *Emcn* or whether the lack of protein expression was due to another cause, such as disturbed post-transcriptional regulation.

4.6 RNA expression

Following isolation of WBM cells and sorting of LT-HSCs from 3 uninduced $Emcn^{fl/fl}$ mice and 3 C57BL/6 mice, RNA was isolated from the cells, and cDNA was synthesized. The samples were run on Lightcycler PCR machine with specific primers used to amplify *Emcn* and *Hprt* cDNA.

Figure 21 show the quantification of the qPCR data demonstrating the level of *Emcn* expression in WBM cells and HSCs relative to the expression of *Hprt* in the sample. The similar level of *Emcn* expression seen in WBM cells and HSCs in the C57BL/6 mice was surprising. Since the HSC population contains a significantly higher frequency of HSCs expressing EMCN, a much more significant difference in the level of *Emcn* transcripts was expected [81]. However, the *Emcn* expression in the targeted mice was much lower than the level of expression in C57BL/6 mice, both in the WBM cells and in the HSCs. The bar chart reveals that the level of *Emcn* expression in the $Emcn^{fl/fl}$ mice was not at detectable levels. This suggested that the lack of EMCN expression in targeted mice was due to interfered transcription of the gene caused by the inserted LoxP sites flanking exon 1.

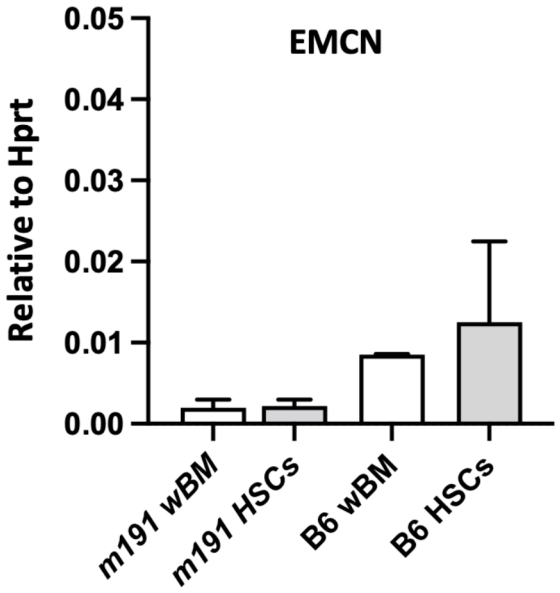

Figure 21: **Quantification of qPCR data demonstrating the level of *Emcn* mRNA expression in *Emcn*$^{fl/fl}$ and C57BL/6 mice.** Mean ± SD expression level of *Emcn* transcripts relative to the expression of *Hprt* in WBM cells and HSCs from *Emcn*$^{fl/fl}$ and C57BL/6 mice. The level of *Emcn* mRNA in WBM cells and HSCs from *Emcn*$^{fl/fl}$ mice is close to 0, and much lower compared to the level in WBM cells and HSCs from C57BL/6 mice. C57BL/6: n=3, *Emcn*$^{fl/fl}$: n=3.

5 Discussion

Hematopoietic stem cells are responsible for the lifelong production and replenishment of mature blood cells. This is accomplished by their defining capacity to balance self-renewal and differentiation, enabling the maintenance of the HSC pool while ensuring sufficient production of all hematopoietic lineages [3].

This project was carried out to investigate the function of EMCN in murine LT-HSCs, eventually aiming to explore the function of EMCN as a new LT-HSC marker. EMCN is a type I integral membrane O-sialoglycoprotein, initially identified in murine and human endothelial cells [85], where it has been shown to be essential for the negative regulation of adhesion to other cells [87], as well as for angiogenesis [86]. However, in later studies, its presence on murine and human HSCs, as well as its moderate/low expression level on more differentiated cells, were confirmed [82] [83]. Additionally, EMCN is not expressed by AML cancer cells, in contrast to CD34 [81], which is currently used as a marker to assess and purify HSCs for stem cell transplantation of patients with AML and other blood disorders [80]. Therefore, establishing EMCN as a novel HSC marker appears to be particularly promising for the treatment of AML. Owing to the promising implication of EMCN as a marker for purging autologous grafts from contaminating cancer cells (that may be $CD34^+$), Kristian Reckzeh and other colleagues in the Finsen lab managed to show that EMCN enriches for human HSCs, and that only cells expressing this marker have the capacity for human long-term multilineage engraftment [83]. Following these findings, Ph.D. student Sophia Engelhard defined EMCN as a marker of murine HSCs, demonstrating that EMCN enriches for murine LT-HSCs and that $EMCN^+$ LT-HSCs have a higher engraftment capacity than $EMCN^-$ LT-HSCs (unpublished data by Sophia Engelhard, Kristian Reckzeh, and Kim Theilgaard-Mönch). The fact that EMCN, opposite to most of the current HSC markers, is conserved between mice and humans is highly advantageous since it allows for the use of mouse models to perform functional genetic studies of the protein [82]. A conventional EMCN KO mouse model was designed and applied in the lab to study the function of EMCN; however, no protein phenotype has been revealed in this model yet (unpublished data by Sophia Engelhard, Kristian Reckzeh, and Kim Theilgaard-Mönch). However, owing to the previous findings demonstrating the importance of EMCN in hematopoiesis, the novel *Emcn* conditional

KO model used in this project was designed to further investigate the function of EMCN in hematopoiesis.

5.1 No function of EMCN in LT-HSCs could be revealed

The *Emcn* conditional KO model was used to study the functional consequence of EMCN loss in hematopoiesis. However, no phenotype could be revealed, neither in the analysis comparing the polyI:C treated $Emcn^{fl/fl}$;Mx1Cre mice with polyI:C treated $Emcn^{fl/fl}$ mice nor through the transplantation assays. These results suggested that EMCN has no function in hematopoiesis. However, the following analysis of LT-HSCs derived from targeted mice treated with polyI:C and of donor-derived LT-HSCs from recipients in the transplantation assay demonstrated that both mouse models lacked EMCN expression. During the course of experiments, it became evident that the introduction of LoxP sites alongside exon 1 of Emcn resulted in down-regulation of Emcn expression both in the $Emcn^{fl/fl}$;Mx1Cre mice and in the $Emcn^{fl/fl}$ mice. Therefore, no differences between the two investigated groups can be expected. However, despite the lack of a proper control and the unfortunate outcome of the X-ray irradiation, some assumptions that need further investigation can be made from the transplantation assays.

5.1.1 EMCN is not essential for HSCs to differentiate to mature blood cells

Prior to the transplantation assays, blood count analysis of PB from EMCN KO mice was performed using C57BL/6 mice as controls. The analysis revealed that there was no significant difference between the EMCN KO mice and the C57BL/6 mice for any of the parameters analyzed. This indicates that the EMCN activity in HSCs is not essential for their capacity to differentiate to mature lineages. However, in order to draw any conclusion on this matter, a proper EMCN WT control is needed.

5.1.2 EMCN is not crucial for the maintenance of HSC quiescence

Upon sorting EMCN KO LT-HSCs for transplantation, cell cycle analysis addressing cell cycle state in these cells revealed that about 70% of the cells were in G_0 phase. This is notably different from 90-95%, which according to literature, is the normal percentage of

homeostatic HSCs in quiescent state [37]. However, the decreased percentage of quiescent cells might be explained by the polyI:C treatment known to induces an inflammatory state in the mice [97], potentially leading to HSC cell cycle entry [37]. Nevertheless, in a study by Pietras et al., investigating the effect of polyI:C induced IFN-1 in HSCs, it was shown that IFN-1–driven HSC proliferation only is a transient event. They demonstrated a significant decrease in HSC quiescent state after three days of polyI:C treatment, however following polyI:C treatment every second day for 7 days, as applied in this project, the HSC compartment returned to a predominantly quiescent phenotype [101]. This suggests that the low percentage of quiescent EMCN KO HSCs could not be explained by the polyI:C treatment.

To investigate if the relatively low percentage of quiescent LT-HSCs observed in the EMCN KO mice could be explained by the EMCN loss, the cell cycle data were compared to previous data obtained in the lab, generated using the same protocol. Data obtained from comparing cell cycle state in conventional EMCN KO LT-HSCs and C57BL/6 LT-HSCs revealed that the percentage of quiescent LT-HSCs in both mouse models were around 70% (Figure 22), as seen in the *Emcn* conditional KO mice. The data demonstrate that by using this protocol, only about 70% of C57BL/6 LT-HSCs are detected in G_0 phase. This suggests that the relatively low percentage of quiescent conditional EMCN KO LT-HSCs was not caused by the EMCN loss. This idea is also strengthened by the result obtained from the conventional EMCN LT-HSCs, demonstrating similar percentages of quiescent LT-HSCs as in the C57BL/6 mice (Figure 22). Taken together, this indicates that EMCN is not essential for maintaining HSC quiescence.

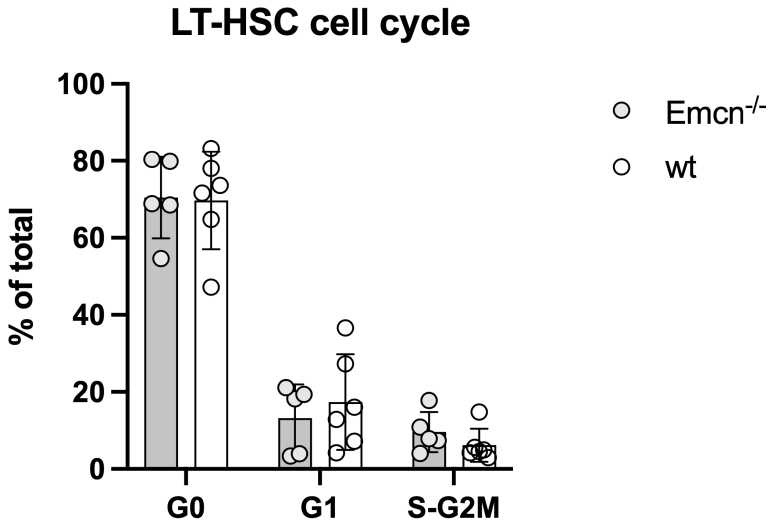

Figure 22: **Cell cycle analysis of conventional EMCN KO LT-HSCs and C57BL/6 LT-HSCs.** Quantified cell cycle FACS data. The bar chart presents the mean ± SD percentage of EMCN$^{-/-}$ (n=5) and EMCN WT (n=6) LT-HSCs in G_0, G_1, and S-G_2M phase of the cell cycle. About 70% of the LT-HSCs are in G_0 phase, about 15% are in G_1 pahse, and about 10% are in S-G_2M phase of cell cycle. Unpublished data by Sophia Engelhard, Kristain Reckzeh, and Kim Theilgaard-Mönch.

5.1.3 The transplantation assays indicate that EMCN is dispensable for the capacity of HSCs to reconstitute the hematopoietic system

Although there was no proper control in this project, the transplantation assays revealed that EMCN KO LT-HSCs can regenerate the hematopoietic system of lethally irradiated recipients. The fact that the recipient mice exhibited donor-derived blood cells of all lineages highly suggests that the HSC defining properties of self-renewal and multilineage engraftment are not dependent on EMCN activity. This is also what has been observed through similar transplantation assays performed with the conventional KO in the Finsen lab, strongly indicating that EMCN is dispensable for the capacity of HSCs to reconstitute the hematopoietic system. However, in order to draw any conclusions, a proper control is needed. A competitive transplantation assay which improves the sensitivity of the transplantation assay should also be performed to confirm the role of EMCN in hematopoiesis.

The results indicating that EMCN is not essential for the repopulating capacity of HSCs counteracts the findings in the study performed by Holmfeldt et al. Upon generating EMCN knock-down HSPCs by treating the cells with shRNA targeted to EMCN and transplanting these cells into ablated mice, they demonstrated that EMCN is required for optimal HSPC repopulation [90]. Considering the counteracting results obtained in the *Emcn* conditional and conventional KO models, further investigation is needed in order to assess the role of EMCN in HSC repopulation.

Furthermore, the results suggesting that EMCN is not crucial for the repopulating capacity of HSCs, challenge the previous findings in the lab demonstrating that cells expressing EMCN have a greater capacity of human [83] and murine long-term multilineage engraftment (unpublished data by Sophia Engelhard, Kristian Reckzeh, and Kim Theilgaard-Mönch). As HCSs and endothelial cells share the common precursor hemangioblast [6], the current findings, in light of the previous discoveries in the lab, suggest that EMCN may be expressed on HSCs as a reminiscent protein expressed during early hematopoietic development by the hemangioblast. However, since this project only assessed the role of EMCN in HSC self-renewal and multipotency, it cannot be ruled out that EMCN may be essential for HSC homing and migration, as well as for adhesion, as seen in endothelial cells.

5.2 The X-ray irradiation caused severe lesions on the mice

Since the Gammacell irradiator, which is usually used in the lab for lethal irradiation of mice, was not available when the transplantation assays were initiated, the mice were irradiated with a X-ray irradiator instead. The X-ray irradiation dose of 9 Gray (1 Gray/minute) caused severe lesions on the neck of the mice leading to the unfortunate sacrifice of 13/42 irradiated mice. This compromised the significance of the transplantation assays performed, and led to the termination of the competitive transplantation assay that was established. Irradiation with a dose of 9 Gray is the standard procedure for lethal gamma-irradiation in the lab. However, upon changing the irradiation source to X-ray, the need for changing the irradiation dose was not considered.

Gamma irradiators emit gamma radiation as a result of radioactive sources and nuclear decay, whereas X-ray irradiators are based on electricity powering X-ray tubes to radiate. It has been reported that the relative biological effect (RBE) of X-ray radiation, is 30-40% (measured in Gray) greater than that of gamma radiation. This means that a lower dose of X-ray radiation can be applied to reach the same biological effect as a higher dose of gamma radiation [102]. Comparing the effect of X-ray irradiation with the effect of gamma irradiation on mice, Gibson et al. managed to show that X-ray irradiation is associated with higher overall morbidity and that the different radiation sources result in distinct physiologic responses [103]. Due to these circumstances, the lab has now decided to lower the X-ray irradiation dose. Upon using the X-ray irradiator for lethal irradiation of mice in the future, the radiation dose should be reduced to 8.50 Gray, with a rate of 0.7 Gray/minute.

5.3 LoxP sites along *Emcn* exon 1 interferes with gene transcription

The disclosure of the EMCN deficient $Emcn^{fl/fl}$ mice was highly in conflict with the genotyping results showing that *Emcn* was not knocked out at the gene level in these mice. However, demonstrating that targeted mice neither expressed EMCN protein nor its transcript, regardless of whether the KO was induced, highly indicated that the inserted LoxP sites had interfered with the expression of the gene.

Following these findings, we were informed by the transgenic mouse facility that designed the model that the sequence upstream of exon 1, where one of the LoxP sites was inserted, was part of the flanking region of a promotor essential for *Emcn* transcription [104]. However, the importance of this sequence was not yet discovered at the time when the model was generated. The lab is now in contact with the transgenic mouse facility regarding the generation of a new *Emcn* conditional KO model with another target exon for assessment of the role of EMCN in hematopoiesis.

5.4 Future perspectives

Since the target strategy applied to generate the *Emcn* conditional KO model used in this project proved to interfere with *Emcn* gene expression, a new conditional model should be designed to investigate the function of EMCN in hematopoiesis. Even though the transplantation assays suggest that EMCN is not essential for the HSCs' capacity to reconstitute the hematopoietic system, experiments need to be repeated with a proper EMCN WT control. Additionally, to rule out the function of EMCN in HSCs and hematopoiesis, its potential role in homing, migration, and adhesion should be investigated.

To investigate EMNS's role in migration, EMCN KO and EMCN WT mice can be treated with granulocyte-colony stimulating factor (G-CSF). This cytokine facilitates the migration of HSCs from the BM niche to the vessels. G-CSF is also applied in the clinic to mobilize HSCs into PB upon harvesting cells for transplantation purposes. Upon treatment with G-CSF, the migration capacity of the EMCN KO and EMCN WT HSCs can be assessed by measuring the frequency of HSCs in the blood [105]. To study HSC homing capacity, fluorescent dyes, e.g., carboxyfluorescein diacetate succinimidyl ester (CFSE), can be applied to evaluate the ability of HSCs transplanted into the blood to home in the BM cavity. Following transplantation of $CFSE^+$ EMCN KO or EMCN WT HSCs, homing capacity can be assessed by measuring the ratio of $CFSE^+$ donor cells in the BM, divided by the total number of HSCs transplanted [106]. Finally, the HSCs capacity to adhere to other BM cells in their niche are believed to regulate HSC self-renewal, and differentiation [107]. The function of EMCN in HSC adhesioin could be assessed through monitoring growth of EMCN KO or EMCN WT HSCs cultured in vitro on EMCN KO stromal cells, or EMCN WT stromal cells. However, in order to investigate the function of EMCN in HSC homing, migration, and adhesion in *Emcn* conditional KO mice, a new model must be generated.

Designing a new *Emcn* conditional KO model, floxing exon 2 with LoxP sites could be a promising approach, given its early positioning in the gene. Following polyI:C treatment, the knock-out of exon 2 will hopefully lead to a frameshift deletion. Frameshift mutations alter the amino acid reading frame, which normally leads to the introduction of premature termination codons. Premature termination generally leads to truncated

protein outcomes [108] or complete KO, resulting from degraded mRNA [109]. The KO of *Emcn* exon 2 will expectantly lead to a non-functional EMCN protein. However, since the function of EMCN is not known, the persisted part of EMCN in a truncated protein, coded by exon 1, might be active in intracellular signaling, even if the protein cannot bind to the membrane. Therefore, both surface and intracellular protein expression should be tested, e.g., by FACS and Western blot, respectively, prior to using this model for research.

6 Conclusion

.

This project was carried out to explore the function of EMCN in LT-HSCs, eventually aiming to functionally characterize EMCN as a new LT-HSC marker. Unfortunately, the strategy applied to generate the conditional EMCN KO model interfered with EMCN gene expression. This resulted in the lack of a proper WT control in the assays performed. Due to this, the analysis comparing the EMCN KO mice to EMCN WT mice was inconclusive. However, despite the lack of control mice, the transplantation assays performed indicate that EMCN KO LT-HSCs are capable of reconstituting the hematopoietic system of lethally irradiated mice. This suggests that EMCN is dispensable for HSC self-renewal and differentiation, which is critical for their repopulating capacity. Nevertheless, in order to conclude on the function of EMCN in hematopoiesis, the analyses need to be repeated with a proper EMCN KO control. This can be accomplished by the generation of a new conditional knockout model for EMCN, targeting exon 2 with LoxP sites. This model would hopefully allow proper investigation of the effect of EMCN on mature blood cell production, the cell cycle, and the HSCs' ability to reestablish the hematopoietic system of the lethally irradiated mice. Additionally, in order to fully explore the function of EMCN in HSCs, its role in migration, homing, and adhesion should be assessed.

References

[1] Orkin SH, Zon LI. Hematopoiesis: an evolving paradigm for stem cell biology. Cell. 2008;132(4):631-44.

[2] Olsen AL, Stachura DL, Weiss MJ. Designer blood: creating hematopoietic lineages from embryonic stem cells. Blood. 2006;107(4):1265-75.

[3] Orkin SH. Diversification of haematopoietic stem cells to specific lineages. Nature Reviews Genetics. 2000;1(1):57-64.

[4] Shizuru JA, Negrin RS, Weissman IL. Hematopoietic stem and progenitor cells: clinical and preclinical regeneration of the hematolymphoid system. Annu Rev Med. 2005;56:509-38.

[5] Eaves CJ. Hematopoietic stem cells: concepts, definitions, and the new reality. Blood, The Journal of the American Society of Hematology. 2015;125(17):2605-13.

[6] Jagannathan-Bogdan M, Zon LI. Hematopoiesis. Development. 2013;140(12):2463-7.

[7] Morcos MN, Zerjatke T, Glauche I, Munz CM, Ge Y, Petzold A, et al. Continuous mitotic activity of primitive hematopoietic stem cells in adult mice. Journal of Experimental Medicine. 2020;217(6).

[8] Gordon-Smith T. Structure and function of red and white blood cells. Medicine. 2013;41(4):193-9.

[9] Holinstat M. Normal platelet function. Cancer and Metastasis Reviews. 2017;36(2):195-8.

[10] Blumenreich MS. The white blood cell and differential count. Clinical Methods: The History, Physical, and Laboratory Examinations 3rd edition. 1990.

[11] Van L, et al. The life span of red cells in the rat and the mouse as determined by labeling with DFP32 in vivo. Blood. 1958;13:789-94.

[12] Pillay J, Den Braber I, Vrisekoop N, Kwast LM, De Boer RJ, Borghans JA, et al. In vivo labeling with 2H2O reveals a human neutrophil lifespan of 5.4 days. Blood, The Journal of the American Society of Hematology. 2010;116(4):625-7.

[13] Valli V, Kiupel M, Bienzle D, Wood RD. Hematopoietic system. Jubb, Kennedy, and Palmer's pathology of domestic animals. 2015;3:102-268.

[14] Nombela-Arrieta C, Manz MG. Quantification and three-dimensional microanatomical organization of the bone marrow. Blood advances. 2017;1(6):407-16.

[15] Mayani H. The regulation of hematopoietic stem cell populations. F1000Research. 2016;5.

[16] Mumau MD, Vanderbeck AN, Lynch ED, Golec SB, Emerson SG, Punt JA. Identification of a multipotent progenitor population in the spleen that is regulated by NR4A1. The Journal of Immunology. 2018;200(3):1078-87.

[17] Weiskopf K, Schnorr PJ, Pang WW, Chao MP, Chhabra A, Seita J, et al. Myeloid cell origins, differentiation, and clinical implications. Myeloid Cells in Health and Disease: A Synthesis. 2017:857-75.

[18] Akashi K, Reya T, Dalma-Weiszhausz D, Weissman IL. Lymphoid precursors. Current opinion in immunology. 2000;12(2):144-50.

[19] De Graaf CA, Choi J, Baldwin TM, Bolden JE, Fairfax KA, Robinson AJ, et al. Haemopedia: an expression atlas of murine hematopoietic cells. Stem cell reports. 2016;7(3):571-82.

[20] Schmitt CE, Lizama CO, Zovein AC. From transplantation to transgenics: mouse models of developmental hematopoiesis. Experimental hematology. 2014;42(8):707-16.

[21] Challen GA, Boles N, Lin KYK, Goodell MA. Mouse hematopoietic stem cell identification and analysis. Cytometry Part A: The Journal of the International Society for Advancement of Cytometry. 2009;75(1):14-24.

[22] Yeung J, So WE, et al. Identification and characterization of hematopoietic stem and progenitor cell populations in mouse bone marrow by flow cytometry. In: Leukemia. Springer; 2009. p. 301-15.

[23] Termini CM, Pang A, Li M, Fang T, Chang VY, Chute JP. Syndecan-2 enriches for hematopoietic stem cells and regulates stem cell repopulating capacity. Blood, The Journal of the American Society of Hematology. 2022;139(2):188-204.

[24] Lai L, Alaverdi N, Maltais L, Morse HC. Mouse cell surface antigens: nomenclature and immunophenotyping. The Journal of Immunology. 1998;160(8):3861-8.

[25] Rossi L, Challen GA, Sirin O, Lin KKY, Goodell MA. Hematopoietic stem cell characterization and isolation. Stem Cell Migration. 2011:47-59.

[26] Kiel MJ, Radice GL, Morrison SJ. Lack of evidence that hematopoietic stem cells depend on N-cadherin-mediated adhesion to osteoblasts for their maintenance. Cell stem cell. 2007;1(2):204-17.

[27] Oguro H, Ding L, Morrison SJ. SLAM family markers resolve functionally distinct subpopulations of hematopoietic stem cells and multipotent progenitors. Cell stem cell. 2013;13(1):102-16.

[28] Wilkerson MJ. Principles and applications of flow cytometry and cell sorting in companion animal medicine. Veterinary Clinics: Small Animal Practice. 2012;42(1):53-71.

[29] Brown M, Wittwer C. Flow cytometry: principles and clinical applications in hematology. Clinical chemistry. 2000;46(8):1221-9.

[30] Reggeti F, Bienzle D. Flow cytometry in veterinary oncology. Veterinary pathology. 2011;48(1):223-35.

[31] Telford WG. Lasers in flow cytometry. Methods in cell biology. 2011;102:373-409.

[32] Kiel MJ, Yilmaz ÖH, Iwashita T, Yilmaz OH, Terhorst C, Morrison SJ. SLAM family receptors distinguish hematopoietic stem and progenitor cells and reveal endothelial niches for stem cells. cell. 2005;121(7):1109-21.

[33] Mikkola HK, Orkin SH. The journey of developing hematopoietic stem cells. 2006.

[34] Huang X, Cho S, Spangrude GJ. Hematopoietic stem cells: generation and self-renewal. Cell Death & Differentiation. 2007;14(11):1851-9.

[35] Kurre P. Balancing the Stem Cell Budget. The Hematologist. 2013;10(3).

[36] Kumar S, Geiger H. HSC niche biology and HSC expansion ex vivo. Trends in molecular medicine. 2017;23(9):799-819.

[37] Pietras EM, Warr MR, Passegué E. Cell cycle regulation in hematopoietic stem cells. Journal of Cell Biology. 2011;195(5):709-20.

[38] Hao S, Chen C, Cheng T. Cell cycle regulation of hematopoietic stem or progenitor cells. International journal of hematology. 2016;103(5):487-97.

[39] Nakamura-Ishizu A, Takizawa H, Suda T. The analysis, roles and regulation of quiescence in hematopoietic stem cells. Development. 2014;141(24):4656-66.

[40] Forsberg EC, Prohaska SS, Katzman S, Heffner GC, Stuart JM, Weissman IL. Differential expression of novel potential regulators in hematopoietic stem cells. PLoS genetics. 2005;1(3):e28.

[41] Morrison SJ, Scadden DT. The bone marrow niche for haematopoietic stem cells. Nature. 2014;505(7483):327-34.

[42] Isern J, Méndez-Ferrer S. Stem cell interactions in a bone marrow niche. Current osteoporosis reports. 2011;9(4):210-8.

[43] Lilly AJ, Johnson WE, Bunce CM. The haematopoietic stem cell niche: new insights into the mechanisms regulating haematopoietic stem cell behaviour. Stem cells international. 2011;2011.

[44] Suda T, Takubo K, Semenza GL. Metabolic regulation of hematopoietic stem cells in the hypoxic niche. Cell stem cell. 2011;9(4):298-310.

[45] Li J. Quiescence regulators for hematopoietic stem cell. Experimental hematology. 2011;39(5):511-20.

[46] Hurwitz SN, Jung SK, Kurre P. Hematopoietic stem and progenitor cell signaling in the niche. Leukemia. 2020;34(12):3136-48.

[47] Calvi L, Adams G, Weibrecht K, Weber J, Olson D, Knight M, et al. Osteoblastic cells regulate the haematopoietic stem cell niche. Nature. 2003;425(6960):841-6.

[48] Blank U, Karlsson S. The role of Smad signaling in hematopoiesis and translational hematology. Leukemia. 2011;25(9):1379-88.

[49] Aleem E, Arceci RJ. Targeting cell cycle regulators in hematologic malignancies. Frontiers in cell and developmental biology. 2015;3:16.

[50] Morgan DO. Cyclin-dependent kinases: engines, clocks, and microprocessors. Annual review of cell and developmental biology. 1997;13(1):261-91.

[51] Matsumoto A, Takeishi S, Kanie T, Susaki E, Onoyama I, Tateishi Y, et al. p57 is required for quiescence and maintenance of adult hematopoietic stem cells. Cell stem cell. 2011;9(3):262-71.

[52] Jaiswal S, Ebert BL. Clonal hematopoiesis in human aging and disease. Science. 2019;366(6465):eaan4673.

[53] Welch JS, Ley TJ, Link DC, Miller CA, Larson DE, Koboldt DC, et al. The origin and evolution of mutations in acute myeloid leukemia. Cell. 2012;150(2):264-78.

[54] Bowman RL, Busque L, Levine RL. Clonal hematopoiesis and evolution to hematopoietic malignancies. Cell stem cell. 2018;22(2):157-70.

[55] Young AL, Tong RS, Birmann BM, Druley TE. Clonal hematopoiesis and risk of acute myeloid leukemia. haematologica. 2019;104(12):2410.

[56] Jaiswal S, Fontanillas P, Flannick J, Manning A, Grauman PV, Mar BG, et al. Age-related clonal hematopoiesis associated with adverse outcomes. New England Journal of Medicine. 2014;371(26):2488-98.

[57] Döhner H, Weisdorf DJ, Bloomfield CD. Acute myeloid leukemia. New England Journal of Medicine. 2015;373(12):1136-52.

[58] Tenen DG. Disruption of differentiation in human cancer: AML shows the way. Nature reviews cancer. 2003;3(2):89-101.

[59] Davis A, Viera AJ, Mead MD. Leukemia: an overview for primary care. American family physician. 2014;89(9):731-8.

[60] Lowenberg B, Downing JR, Burnett A. Acute myeloid leukemia. New England Journal of Medicine. 1999;341(14):1051-62.

[61] Saultz JN, Garzon R. Acute myeloid leukemia: a concise review. Journal of clinical medicine. 2016;5(3):33.

[62] Robak T, Wierzbowska A. Current and emerging therapies for acute myeloid leukemia. Clinical therapeutics. 2009;31:2349-70.

[63] Finn L, Dalovisio A, Foran J. Older patients with acute myeloid leukemia: treatment challenges and future directions. Ochsner Journal. 2017;17(4):398-404.

[64] Duarte RF, Labopin M, Bader P, Basak GW, Bonini C, Chabannon C, et al. Indications for haematopoietic stem cell transplantation for haematological diseases, solid tumours and immune disorders: current practice in Europe, 2019. Bone marrow transplantation. 2019;54(10):1525-52.

[65] Hatzimichael E, Tuthill M. Hematopoietic stem cell transplantation. Stem cells and cloning: advances and applications. 2010;3:105.

[66] Deeg HJ. Allogeneic and autologous bone-marrow transplantation. Canadian Family Physician. 1988;34:2489.

[67] Khaddour K, Hana CK, Mewawalla P. Hematopoietic stem cell transplantation. In: StatPearls [internet]. StatPearls Publishing; 2021. .

[68] Roboz GJ. Current treatment of acute myeloid leukemia. Current opinion in oncology. 2012;24(6):711-9.

[69] Lorenz E, Uphoff D, Reid T, Shelton E. Modification of irradiation injury in mice and guinea pigs by bone marrow injections. Journal of the National Cancer Institute. 1951;12(1):197-201.

[70] Barnes D, Corp M, Loutit J, Neal F. Treatment of murine leukaemia with x rays and homologous bone marrow. British medical journal. 1956;2(4993):626.

[71] Copelan EA. Hematopoietic stem-cell transplantation. New England Journal of Medicine. 2006;354(17):1813-26.

[72] Saulnier N, Di Campli C, Zocco MA, Di Gioacchino G, Novi M, Gasbarrini A. From stem cell to solid organ. Bone marrow, peripheral blood or umbilical cord blood as favorable source? European Review for Medical and Pharmacological Sciences. 2005;9(6):315.

[73] Thomas ED. Landmarks in the development of hematopoietic cell transplantation. World journal of surgery. 2000;24(7):815-8.

[74] Demirci S, Leonard A, Tisdale JF. Hematopoietic stem cells from pluripotent stem cells: Clinical potential, challenges, and future perspectives. Stem Cells Translational Medicine. 2020;9(12):1549-57.

[75] Mosaad Y. Clinical role of human leukocyte antigen in health and disease. Scandinavian journal of immunology. 2015;82(4):283-306.

[76] Vogelsang GB, Lee L, Bensen-Kennedy DM. Pathogenesis and treatment of graft-versus-host disease after bone marrow transplant. Annual review of medicine. 2003;54(1):29-52.

[77] Dickinson AM, Norden J, Li S, Hromadnikova I, Schmid C, Schmetzer H, et al. Graft-versus-leukemia effect following hematopoietic stem cell transplantation for leukemia. Frontiers in immunology. 2017;8:496.

[78] Champlin R. Selection of autologous or allogeneic transplantation. Holland-Frei cancer medicine. 2003.

[79] Wognum AW, Eaves AC, Thomas TE. Identification and isolation of hematopoietic stem cells. Archives of medical research. 2003;34(6):461-75.

[80] Hassan H, Zeller W, Stockschläder M, Krüger W, Hoffknecht M, Zander A. Comparison between bone marrow and G-CSF-mobilized peripheral blood allografts undergoing clinical scale CD34+ cell selection. Stem cells. 1996;14(4):419-29.

[81] Bagger FO, Sasivarevic D, Sohi SH, Laursen LG, Pundhir S, Sønderby CK, et al. BloodSpot: a database of gene expression profiles and transcriptional programs for healthy and malignant haematopoiesis. Nucleic acids research. 2016;44(D1):D917-24.

[82] Matsubara A, Iwama A, Yamazaki S, Furuta C, Hirasawa R, Morita Y, et al. Endomucin, a CD34-like sialomucin, marks hematopoietic stem cells throughout development. The Journal of experimental medicine. 2005;202(11):1483-92.

[83] Reckzeh K, Kizilkaya H, Helbo AS, Alrich ME, Deslauriers AG, Grover A, et al. Human adult HSCs can be discriminated from lineage-committed HPCs by the expression of endomucin. Blood advances. 2018;2(13):1628.

[84] Morgan SM, Samulowitz U, Darley L, Simmons DL, Vestweber D. Biochemical characterization and molecular cloning of a novel endothelial-specific sialomucin. Blood, The Journal of the American Society of Hematology. 1999;93(1):165-75.

[85] Kuhn A, Brachtendorf G, Kurth F, Sonntag M, Samulowitz U, Metze D, et al. Expression of endomucin, a novel endothelial sialomucin, in normal and diseased human skin. Journal of investigative dermatology. 2002;119(6):1388-93.

[86] Zahr A, Alcaide P, Yang J, Jones A, Gregory M, Patel-Hett S, et al. Endomucin prevents leukocyte–endothelial cell adhesion and has a critical role under resting and inflammatory conditions. Nature communications. 2016;7(1):1-10.

[87] Ueno M, Igarashi K, Kimura N, Okita K, Takizawa M, Nobuhisa I, et al. Endomucin is expressed in embryonic dorsal aorta and is able to inhibit cell adhesion. Biochemical and biophysical research communications. 2001;287(2):501-6.

[88] Yang J, LeBlanc ME, Cano I, Saez-Torres KL, Saint-Geniez M, Ng YS, et al. ADAM10 and ADAM17 proteases mediate proinflammatory cytokine-induced and constitutive cleavage of endomucin from the endothelial surface. Journal of Biological Chemistry. 2020;295(19):6641-51.

[89] Park-Windhol C, Ng YS, Yang J, Primo V, Saint-Geniez M, D'Amore PA. Endomucin inhibits VEGF-induced endothelial cell migration, growth, and morphogenesis by modulating VEGFR2 signaling. Scientific reports. 2017;7(1):1-13.

[90] Holmfeldt P, Ganuza M, Marathe H, He B, Hall T, Kang G, et al. Functional screen identifies regulators of murine hematopoietic stem cell repopulation. Journal of Experimental Medicine. 2016;213(3):433-49.

[91] Sung CO, Kim SC, Karnan S, Karube K, Shin HJ, Nam DH, et al. Genomic profiling combined with gene expression profiling in primary central nervous system lymphoma. Blood, The Journal of the American Society of Hematology. 2011;117(4):1291-300.

[92] Dai W, Liu J, Liu B, Li Q, Sang Q, Li YY. Systematical analysis of the cancer genome atlas database reveals EMCN/MUC15 combination as a prognostic signature for gastric cancer. Frontiers in molecular biosciences. 2020;7:19.

[93] Bao B, Zheng C, Yang B, Jin Y, Hou K, Li Z, et al. Identification of subtype-specific three-gene signature for prognostic prediction in diffuse type gastric cancer. Frontiers in oncology. 2019;9:1243.

[94] Gu H, Marth JD, Orban PC, Mossmann H, Rajewsky K. Deletion of a DNA polymerase β gene segment in T cells using cell type-specific gene targeting. Science. 1994;265(5168):103-6.

[95] Velasco-Hernandez T, Säwén P, Bryder D, Cammenga J. Potential pitfalls of the Mx1-Cre system: implications for experimental modeling of normal and malignant hematopoiesis. Stem cell reports. 2016;7(1):11-8.

[96] Friedel RH, Wurst W, Wefers B, Kühn R. Generating conditional knockout mice. In: Transgenic Mouse Methods and Protocols. Springer; 2011. p. 205-31.

[97] Gudmundsson KO, Oakley K, Han Y, Du Y. Analyzing gene function in adult long-term hematopoietic stem cells using the interferon inducible Mx1-Cre mouse system. In: Mouse Genetics. Springer; 2014. p. 313-25.

[98] Kühn R, Schwenk F, Aguet M, Rajewsky K. Inducible gene targeting in mice. Science. 1995;269(5229):1427-9.

[99] Kim KH, Sederstrom JM. Assaying cell cycle status using flow cytometry. Current protocols in molecular biology. 2015;111(1):28-6.

[100] Kwarteng EO, Heinonen KM. Competitive transplants to evaluate hematopoietic stem cell fitness. JoVE (Journal of Visualized Experiments). 2016;(114):e54345.

[101] Pietras EM, Lakshminarasimhan R, Techner JM, Fong S, Flach J, Binnewies M, et al. Re-entry into quiescence protects hematopoietic stem cells from the killing effect of chronic exposure to type I interferons. Journal of Experimental Medicine. 2014;211(2):245-62.

[102] Storer JB, Harris PS, Furchner JE, Langham WH. The relative biological effectiveness of various ionizing radiations in mammalian systems. Radiation Research. 1957;6(2):188-288.

[103] Gibson BW, Boles NC, Souroullas GP, Herron AJ, Fraley JK, Schwiebert RS, et al. Comparison of cesium-137 and X-ray irradiators by using bone marrow transplant reconstitution in C57BL/6J mice. Comparative medicine. 2015;65(3):165-72.

[104] Cunningham F, Allen JE, Allen J, Alvarez-Jarreta J, Amode MR, Armean IM, et al. Ensembl 2022. Nucleic acids research. 2022;50(D1):D988-95.

[105] Winkler IG, Wiercinska E, Barbier V, Nowlan B, Bonig H, Levesque JP. Mobilization of hematopoietic stem cells with highest self-renewal by G-CSF precedes clonogenic cell mobilization peak. Experimental hematology. 2016;44(4):303-14.

[106] Heazlewood SY, Oteiza A, Cao H, Nilsson SK. Analyzing hematopoietic stem cell homing, lodgment, and engraftment to better understand the bone marrow niche. Annals of the New York Academy of Sciences. 2014;1310(1):119-28.

[107] Geiger H, Koehler A, Gunzer M. Stem cells, aging, niche, adhesion and Cdc42: a model for changes in cell-cell interactions and hematopoietic stem cell aging. Cell Cycle. 2007;6(8):884-7.

[108] Mort M, Ivanov D, Cooper DN, Chuzhanova NA. A meta-analysis of nonsense mutations causing human genetic disease. Human mutation. 2008;29(8):1037-47.

[109] Hentze MW, Kulozik AE. A perfect message: RNA surveillance and nonsense-mediated decay. Cell. 1999;96(3):307-10.

7 Appendix

7.1 Appendix 1: 10x Phosphate Buffered Saline (PBS) (1000 mL)

Components	**Amount**
Na_2HPO_4	10 47.2 g
NaH_2PO_4	26.4 g
NaCl	58.4 g
ddH_2O	Up to 1000 mL

7.2 Appendix 2: Supplementary figures

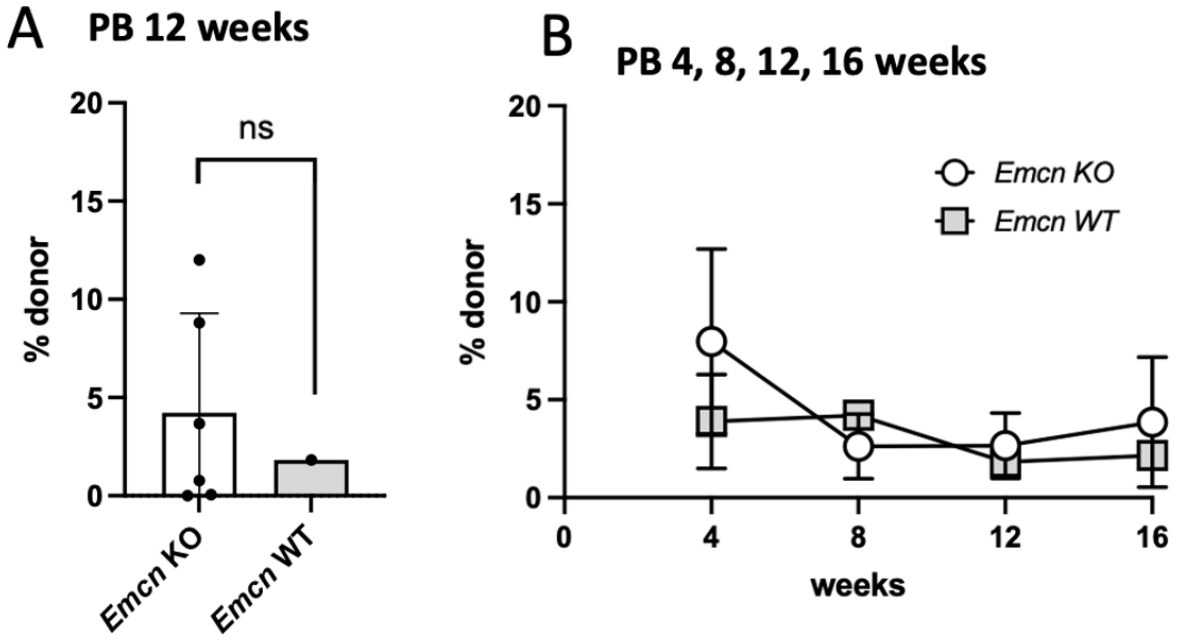

Supplementary Figure 1: **Quantification of FACS analysis of PB during LT-HSC transplantation assay - exp.1.** **(A)** Quantification of FACS analysis for donor derived PB cells in recipient mice from exp. 1- 12 weeks after transplantation. The graph shows the mean ± SEM of the percentage of donor derived PB cells in recipient mice transplanted with EMCN KO and EMCN WT LT-HSCs. About 2-5% of the PB cells in the recipient mice were donor derived. T-test shows no significant difference in the percentage of donor derived PB cells between the two groups of recipients. **(B)** Quantified FACS data for donor derived PB cells in recipient mice in epx. 1 - 4, 8, 12, and 16 weeks post transplantation. The graph shows the mean ± SEM of the percentage of donor derived PB cells as a function of time. EMCN KO (n=6), EMCN WT LT-HSCs (n=1).

NTNU
Norwegian University of
Science and Technology